A. MOHAMMAD ARIF

HYDROTHERMAL SYNTHESIS AND CHARACTERIZATION OF ZNO NANOPARTICLES

THE GRADUATE SCHOOL OF NATURAL AND APPLIED SCIENCES
OF
ATILIM UNIVERSITY

AHMED MOHAMMAD ARIF

A MASTER OF SCIENCE THESIS
IN
THE DEPARTMENT OF PHYSICS

JULY 2025

ATILIM UNIVERSITY 2025

HYDROTHERMAL SYNTHESIS AND CHARACTERIZATION OF ZNO NANOPARTICLES

A THESIS SUBMITTED TO
THE GRADUATE SCHOOL OF NATURAL AND APPLIED SCIENCES
OF
ATILIM UNIVERSITY

BY

AHMED MOHAMMAD ARIF

IN PARTIAL FULFILLMENT OF THE REQUIREMENTS
FOR
THE DEGREE OF MASTER OF SCIENCE
IN
THE DEPARTMENT OF PHYSICS

JULY 2025

Approval of the Graduate School of Natural and Applied Sciences, Atılım University.

_____

Assoc. Prof. Dr. Gökhan TUNÇ
Director

I certify that this thesis satisfies all the requirements as a thesis for the degree of **Master of Science in Physics, Atılım University**.

_____

Prof. Dr. Filiz KORKMAZ ÖZKAN
Head of Department

This is to certify that we have read the thesis HYDROTHERMAL SYNTHESIS AND CHARACTERIZATION OF ZNO NANOPARTICLES submitted by AHMED MOHAMMAD ARIF and that in our opinion it is fully adequate, in scope and quality, as a thesis for the degree of Master of Science.

_____

Assoc. Prof. Dr. Özge SÜRÜCÜ
Supervisor

Examining Committee Members:

Assist. Prof. Dr. Yeliz AKPINAR
Dept. of Chemistry., Kırşehir Ahi Evran University _____

Assoc. Prof. Dr. Özge SÜRÜCÜ
Dept. of Electrical-Electronics Eng., Atılım University_____

Assist. Prof. Dr. Neslihan GÖKÇEK
Dept. of Electrical-Electronics Eng., Atılım University_____

Date: *July 1, 2025*

I hereby declare that all information in this document has been obtained and presented in accordance with academic rules and ethical conduct. I also declare that, as required by these rules and conduct, I have fully cited and referenced all material and results that are not original to this work.

Name, Last Name: Ahmed MOHAMMAD ARIF

Signature:

ABSTRACT

HYDROTHERMAL SYNTHESIS AND CHARACTERIZATION OF ZNO NANOPARTICLES

Mohammad Arif, Ahmed
Master, Department of Physics
Supervisor: Assoc. Prof. Dr. Özge Sürücü

July 2025, 49 pages

This thesis examines the hydrothermal synthesis of ZnO nanoparticles, emphasizing the effect of reaction duration on their structural, morphological, optical, and colloidal properties. ZnO nanoparticles were synthesized over different time periods—5, 15, 25, and 35 hours. The synthesized materials were comprehensively characterized using X-ray Diffraction (XRD), Scanning Electron Microscopy (SEM), Raman Spectroscopy, Photoluminescence (PL) Spectroscopy, and Zeta Potential analysis. XRD analysis confirmed the successful formation of the hexagonal wurtzite ZnO phase in all samples, with crystallinity increasing with synthesis time. SEM images showed morphology evolving from dense flower-like aggregates at 5 hours to dispersed rod-like particles at 35 hours, highlighting reaction time as a key factor. Raman spectroscopy confirmed high crystallinity and wurtzite structure, while zeta potentials (~ -25 mV) indicated stable colloidal behavior, independent of synthesis duration. Photoluminescence analysis identified a strong, defect-related emission in the near-infrared region (~740-745 nm), with the emission intensity peaking for the 25-hour sample, suggesting an optimal balance between crystal quality and radiative defect density.

Keywords: Zinc oxide nanoparticles, Hydrothermal synthesis, Characterization, Morphology evolution, Photoluminescence

ÖZ

ZNO NANOPARÇACIKLARININ HİDROTERMAL SENTEZİ VE KARAKTERİZASYONU

Mohammad Arif, Ahmed

Yüksek Lisans, Fizik Bölümü

Tez Yöneticisi: Doç. Dr. Özge Sürücü

Temmuz 2025, 49 sayfa

Bu tezde hidrotermal yöntemle sentezlenen ZnO nanoparçacıkları, sentez süresinin yapısal, morfolojik, optik ve kolloidal özelliklere etkisi açısından incelenmiştir. ZnO nanoparçacıkları 5, 15, 25 ve 35 saatlik sürelerle sentezlenmiştir. Elde edilen örnekler, X-Işını Kırınımı (XRD), Taramalı Elektron Mikroskobu (SEM), Raman Spektroskopisi, Fotolüminesans (PL) Spektroskopisi ve Zeta Potansiyeli analizleri ile kapsamlı olarak karakterize edilmiştir. XRD analizleri tüm örneklerin hekzagonal wurtzite ZnO yapısına sahip olduğunu ve kristalitenin sentez süresiyle arttığını doğrulamıştır. SEM görüntüleri, morfolojinin 5 saatlik sentezde yoğun ve çiçek benzeri agregalardan, 35 saatlik sentezde daha ayrık çubuksu yapılara dönüştüğünü ortaya koymuş, reaksiyon süresinin morfolojiyi belirleyici temel faktör olduğunu göstermiştir. Raman spektroskopisi, yüksek kristaliniteyi ve wurtzite yapısını doğrularken, yaklaşık -25 mV değerindeki zeta potansiyeli sonuçları, sentez süresinden bağımsız olarak nanoparçacıkların kararlı kolloidal davranış sergilediğini ortaya koymuştur. Fotolüminesans analizi, yakın kızılötesi bölgede (~740-745 nm) kuvvetli kusur kaynaklı emisyonu belirlemiş ve 25 saatlik örnekte emisyon şiddetinin maksimuma ulaştığını göstererek kristal kalitesi ve radyatif kusur yoğunluğu arasında optimal bir dengeye işaret etmiştir.

Anahtar Kelimeler: Çinko oksit nanoparçacıkları, Hidrotermal sentez, Karakterizasyon, Morfoloji evrimi, Fotolüminesans

To my parents, family, wife and friends…

ACKNOWLEDGMENTS

Firstly, I would like to express my sincere gratitude to my supervisor, Assoc. Prof. Dr. Özge Sürücü, for her invaluable guidance, continuous support, patience, and encouragement throughout my master's studies. Her insights and expertise have been crucial in the successful completion of this thesis.

I am deeply grateful to Dr. Yeliz Akpınar and Gözde Altuntaş for their generous assistance during the experimental phase of my research. Their support in laboratory studies, experimental design, and access to necessary facilities significantly contributed to my work.

I would also like to extend my sincere thanks to Dr. Neslihan Gökçek for her constructive comments, valuable advice, and thoughtful feedback provided during my thesis defense. Her insights greatly improved the quality of my thesis.

Above all, my deepest love and gratitude go to my beloved mother, whose prayers, love, and sacrifices have been the foundation of my strength and success.

To my dear wife, thank you for your patience, understanding, and unwavering support during the most challenging moments. Your belief in me has kept me going.

I also extend my sincere gratitude to my eldest brother Mr. ABDUSSALAM and my eldest sister, whose wisdom, encouragement, and unconditional support have always inspired and strengthened me. And to my entire family, for their love and continuous support that kept me going

A special thank you to Mr. TAWFEEQ Al-SAYEDI and his honorable father Mr. IBRAHIM for their generous help, guidance, and continuous encouragement.

I am also truly grateful to Mr. OMAR Al-SHWIKAN for his valuable support and sincere motivation.

My warm thanks to Mr. SULAIMAN HABEEB ALLAH for his kindness and the great support he provided throughout this journey

Lastly, my heartfelt thanks to all members of Group AHD Al-WAFAA, whose sincere friendship and moral support have left a lasting impact on my academic journey.

To all of you — thank you from the bottom of my heart.

TABLE OF CONTENTS

LIST OF TABLES

TABLES

LIST OF FIGURES

FIGURES

CHAPTER 1

INTRODUCTION

Zinc oxide (ZnO) nanoparticles (NPs) represent an incredibly versatile and extensively researched class of materials, and this distinction arises predominantly from their distinct structural features, exceptional optical properties, and an extensive array of physicochemical characteristics, which collectively render them highly suitable and advantageous for a multitude of applications that span a wide range of diverse domains and sectors, including but not limited to electronics, medicine, and environmental science [1], [2] . The distinctive characteristics of zinc oxide (ZnO) nanoparticles position them as versatile agents in a multitude of applications, including drug delivery systems, advanced sensors, and efficient photocatalysts across diverse scientific and industrial domains. Their remarkable multifunctionality is not only a testament to their inherent properties, such as high surface area, biocompatibility, and photostability, but also fuels ongoing research and innovation within the realm of nanotechnology. This dynamic exploration underscores the critical role that ZnO nanoparticles play in enhancing scientific knowledge and fostering practical solutions, thereby significantly contributing to advancements in fields ranging from medicine to environmental science [3]. As researchers continue to delve into the potential of these nanoparticles, their implications for improving therapeutic efficacy, developing sensitive detection mechanisms, and facilitating sustainable chemical processes become increasingly evident, marking them as pivotal components in the future of technological progress.

Structurally, ZnO NPs typically exhibit a wurtzite hexagonal crystal structure, as confirmed by X-ray diffraction (XRD) analysis, and possess a wide bandgap of approximately 3.37 eV at room temperature, which is crucial for their semiconductor applications [4], [5], [6]. The unique characteristics of this specific bandgap significantly enhance its applicability across a wide array of optoelectronic devices. This advancement leads to substantial improvements in efficiency and performance in critical areas such as photodetectors, which are essential for converting light into

electrical signals, and photovoltaic cells, which are vital in harnessing solar energy to generate electricity [7]. By optimizing the bandgap properties, these devices can achieve better sensitivity, responsiveness, and overall energy conversion efficiency, thereby driving innovation and progress in various technological sectors [8]. Moreover, the tunable properties of ZnO nanoparticles enable their integration into hybrid systems, enhancing performance in energy storage and conversion applications, as well as in biomedical fields [9]. This adaptability further solidifies their role as key materials in advancing both technology and health sciences. In agriculture, ZnO NPs serve as effective nanofertilizers, enhancing plant growth and crop yields due to their solubility and bioavailability, while also exhibiting antimicrobial properties that protect plants from pathogens[10], [11]. Additionally, ZnO NPs are utilized in dentistry to enhance the antibacterial properties of restorative materials and as coatings for dental implants [12]. The catalytic activity of ZnO NPs, driven by their large surface area and amphoteric nature, makes them suitable for various industrial applications, including as catalysts in chemical reactions[13]. Despite their numerous benefits, the potential toxicity of ZnO NPs, particularly with prolonged exposure, necessitates further investigation to ensure safe application across different fields [14]. Overall, the multifunctional properties of ZnO nanoparticles underscore their potential in advancing technology and improving industrial and biomedical processes.

Zinc oxide (ZnO) nanoparticles can be synthesized through various methods, each offering unique advantages and characteristics. Common synthesis techniques include sol-gel, co-precipitation, thermal decomposition, and hydrothermal processes. [9], [15], [16], [17]. Among these, the hydrothermal method has gained significant attention due to its effectiveness in producing high-quality ZnO nanoparticles with controlled size and morphology [15], [18].

The hydrothermal process is a sophisticated chemical technique that entails the reaction of zinc precursors within an aqueous solution, subjected to elevated temperatures and pressures. This method capitalizes on the unique properties of the solvent, which plays a crucial role in enhancing the nucleation and subsequent growth of nanoparticles[19]. In a hydrothermal environment, the high temperature and pressure conditions promote the solubility of the precursors, allowing for more effective interactions between the reactants. This leads to a more uniform distribution

of particles throughout the solution, minimizing agglomeration and ensuring that the nanoparticles form consistently in size and shape. Moreover, the controlled hydrothermal conditions facilitate the formation of crystalline structures that exhibit desirable physical and chemical properties. These structures can be tailored by adjusting various parameters such as temperature, pressure, and the concentration of the precursors, enabling the synthesis of nanoparticles with specific characteristics suitable for a wide range of applications, including catalysis, electronics, and biomedical fields. Ultimately, the hydrothermal process stands out as a versatile and efficient method for producing high-quality nanoparticles with enhanced performance attributes. The hydrothermal method's ability to yield nanoparticles with tailored properties positions as a leading technique in nanotechnology, particularly for applications in electronics and biomedical fields[17]. As research progresses, optimizing these synthesis parameters will be crucial for harnessing the full potential of ZnO nanoparticles in various innovative applications [19].

The motivation behind using the hydrothermal process for synthesizing ZnO nanoparticles stems from several key factors:

1. **Controlled Morphology and Size**: The hydrothermal method enables precise control over the size and shape of ZnO nanoparticles, which is crucial for tailoring their properties for specific applications.

2. **High Purity**: The process typically results in high-purity nanoparticles, as the aqueous environment minimizes contamination from external sources.

3. **Crystallinity**: Hydrothermal synthesis often yields well-crystallized ZnO nanoparticles, enhancing their optical and electronic properties, which are essential for applications in electronics and photonics.

4. **Scalability**: The hydrothermal method can be scaled up for industrial production, making it a viable option for commercial applications.

5. **Versatility**: This method can accommodate different zinc precursors and additives, allowing researchers to explore various formulations and optimize the synthesis for specific applications.

In conclusion, zinc oxide (ZnO) nanoparticles (NPs) exemplify a remarkable class of materials distinguished by their unique structural attributes, exceptional optical properties, and versatile physicochemical characteristics. These features not only facilitate their integration into a wide array of applications, spanning electronics, medicine, and environmental science, but also underscore their significance in advancing nanotechnology. The multifunctionality of ZnO NPs—evident in their roles as drug delivery systems, advanced sensors, and efficient photocatalysts—highlights their potential to enhance therapeutic efficacy, improve detection mechanisms, and promote sustainable chemical processes. The hydrothermal synthesis method emerges as a particularly effective technique for producing high-quality ZnO nanoparticles, allowing for precise control over their size, morphology, and crystallinity, which are critical for optimizing their performance in various applications. As research continues to explore the capabilities and implications of ZnO nanoparticles, it is imperative to address potential toxicity concerns to ensure safe utilization across diverse fields. Ultimately, the ongoing innovation surrounding ZnO nanoparticles is poised to significantly contribute to technological advancements and practical solutions in both industrial and biomedical contexts.

This thesis aims to explore the fabrication of ZnO nanoparticles using the hydrothermal method, focusing on optimizing the synthesis parameters to achieve nanoparticles with superior characteristics. The study will investigate the influence of temperature, pressure, precursor concentration, and reaction time on the morphology, size, and crystallinity of the obtained ZnO nanoparticles. Furthermore, the thesis will delve into the characterization of the synthesized nanoparticles using various techniques, including X-ray diffraction (XRD), scanning electron microscopy (SEM), and photoluminescence spectroscopy (PL), to elucidate their structural and optical properties. Ultimately, this research seeks to contribute to the growing body of knowledge surrounding ZnO nanoparticles and their synthesis, providing insights that could pave the way for their application in advanced technologies. By understanding the relationship between synthesis conditions and nanoparticle properties, this work aims to refine the hydrothermal process for producing ZnO nanoparticles with tailored functionalities, thereby enhancing their utility in various fields of science and engineering.

CHAPTER 2

THEORETICAL CONSIDERATIONS

The synthesis and characterization of nanomaterials have become central themes in modern materials science due to the unique properties and diverse applications exhibited by materials at the nanoscale. Among various nanostructured materials, zinc oxide (ZnO) nanoparticles stand out for their exceptional optical, electronic, and catalytic properties, which are closely linked to their size, morphology, and crystal structure. Understanding the theoretical foundations behind the formation, growth, and characterization of ZnO nanoparticles is crucial for optimizing their synthesis and tailoring their functionalities for specific applications. This chapter provides a comprehensive theoretical background on the structural features of ZnO, the fundamental principles of hydrothermal synthesis, and the mechanisms governing nanoparticle nucleation and growth. Additionally, it outlines the key characterization techniques used to analyze the structural and optical properties of ZnO nanoparticles, establishing a framework for interpreting the experimental results presented in subsequent chapters.

2.1. Structure and Fundamental Physical Properties of ZnO Nanoparticles

Zinc oxide (ZnO) is classified as a direct wide bandgap semiconductor, which is a member of the II–VI category of compound semiconductors[20]. Under standard environmental conditions, ZnO primarily adopts the hexagonal wurtzite crystalline structure, which is characterized by the space group $P6_3mc$ (see Figure 2.1)[21]. In this specific and meticulously organized structure, each individual Zn^{2+} ion is coordinated in a tetrahedral fashion by a total of four O^{2-} ions, which together result in a complex lattice that is characterized by alternating planes composed of zinc and oxygen atoms that are systematically stacked along the c-axis of the crystal[22]. Furthermore, the absence of a center of symmetry within the wurtzite structure of this compound bestows upon it a set of distinctive piezoelectric and pyroelectric properties, which are not only intriguing but also hold significant importance in the field of solid-state

physics, attracting the attention of researchers and scientists alike[23].

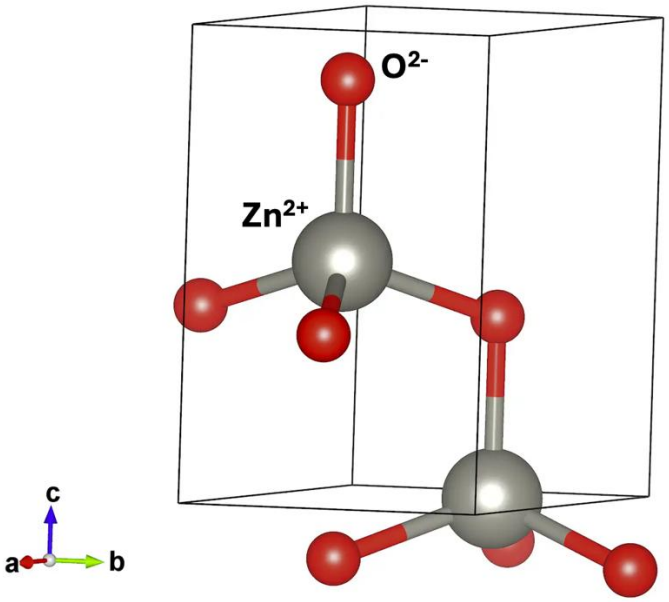

Figure 2.1 The wurtzite crystalline structure of ZnO.

The electronic band structure of bulk ZnO is characterized by a broad and direct bandgap of about 3.37 eV at ambient temperature. The minimum of the conduction band mainly originates from the Zn 4s orbitals, whereas the maximum of the valence band is primarily made up of O 2p orbitals. A significant feature of ZnO is its high exciton binding energy (~60 meV), which allows for the observation of excitonic phenomena even at room temperature. This characteristic is especially important for investigating many-body interactions and exciton dynamics in low-dimensional systems[24].

At the nanoscale, the physicochemical characteristics of ZnO exhibit significant deviations from those of the bulk material as a consequence of quantum confinement phenomena, which become increasingly significant when the dimensions of the nanoparticle approach the Bohr radius of the exciton (approximately 2.34 nm for ZnO). Quantum confinement induces the quantization of electronic energy states, leading to an observable blue shift in both the absorption threshold and photoluminescent emissions. This phenomenon is effectively characterized by models utilizing the

effective mass approximation and has been empirically validated in ZnO nanocrystals with diameters less than approximately 10 nm. As a result, the distinctive attributes of ZnO nanoparticles render them highly viable candidates for a diverse array of applications, encompassing optoelectronic devices, sensing technologies, and ultraviolet light-emitting components[25], [26], [27].

Additionally, the high surface-to-volume ratio of ZnO nanoparticles introduces a substantial number of surface atoms and associated states, which influence their optical, electronic, and chemical properties. The role of intrinsic defects—such as oxygen vacancies (V_O), zinc interstitials (Zn_i), and their complexes—is central in determining the electronic structure and photophysical behavior of ZnO[28]. These defects can introduce localized states within the bandgap, act as donors or acceptors, and affect charge carrier dynamics, recombination processes, and luminescence mechanisms. Detailed investigation of these defect-related phenomena provides valuable insights into solid-state defect physics and the interplay between structure and function in low-dimensional semiconductor systems[29].

A comprehensive understanding and regulation of the structural and physical characteristics of ZnO at the nanoscale are imperative for both foundational inquiries in condensed matter physics and the systematic fabrication of nanomaterials intended for sophisticated technological applications. The subsequent sections delineate a theoretical framework for the synthesis and characterization of ZnO nanoparticles, with a distinct focus on the mechanisms of hydrothermal growth and the fundamental physical principles that underpin them[30].

2.2. Principles of Hydrothermal Synthesis: Thermodynamics and Kinetics

Hydrothermal synthesis represents a prevalent methodology for the fabrication of crystalline oxide nanomaterials, such as ZnO, within meticulously regulated temperature and pressure parameters in aqueous media. Analyzing this process from the vantage point of physical chemistry allows for an exploration of thermodynamic stability, phase equilibria, as well as the kinetics of nucleation and growth.

2.2.1. Thermodynamics of ZnO Formation in Hydrothermal Conditions

The driving force for ZnO crystallization in hydrothermal environments is the supersaturation of zinc and oxygen species in solution. At elevated temperatures and pressures, water acts as both a solvent and a reactant, promoting the hydrolysis of zinc salts (such as $Zn(NO_3)_2$ or $Zn(CH_3COO)_2$) and the subsequent formation of $Zn(OH)_2$ intermediates. The overall reaction can be represented as:

$$Zn^{2+} + 2OH^- \rightarrow Zn(OH)_2 \rightarrow ZnO + H_2O \tag{2.1}$$

The solubility of ZnO is a function of temperature, pressure, and solution pH. Under hydrothermal conditions, the free energy change (ΔG) for the formation of ZnO becomes negative, favoring spontaneous nucleation and crystal growth. The interplay between chemical potential, solubility product (K_{sp}), and the degree of supersaturation governs the phase stability and the onset of nucleation[31], [32].

2.2.2. Classical Nucleation Theory and Nanoscale Formation

The initial stage of nanoparticle formation is described by classical nucleation theory (CNT), which balances the bulk free energy gain of forming a new phase against the surface energy cost of creating a new interface. The critical radius r_c for stable nucleus formation is given by[33]:

$$r_c = \frac{2\gamma V_m}{k_B T ln(S)} \tag{2.2}$$

where γ is the surface energy, V_m is the molar volume, k_B is Boltzmann's constant, T is temperature, and S is the supersaturation ratio. When the system exceeds the critical supersaturation, homogeneous nucleation becomes possible, resulting in the formation of nanoscale ZnO nuclei[34].The kinetics of nucleation can also be influenced by factors such as temperature, pressure, and the presence of additives, which can alter the growth rates and final morphology of ZnO nanoparticles.

2.2.3. Growth Mechanisms: Kinetics and Morphological Control

Following nucleation, nanoparticle growth is primarily governed by the rate of mass transport and surface reaction kinetics. In the hydrothermal process, the supply of Zn^{2+} and OH^- ions, as well as the presence of structure-directing agents (such as HMTA), can selectively influence the relative growth rates of different crystallographic facets. For wurtzite ZnO, the (0001) plane typically exhibits the fastest growth, often resulting in rod-like or columnar morphologies[35].

Particle growth may proceed via two principal mechanisms: (i) diffusion-limited growth, where the supply of reactants to the nucleus surface is rate-limiting, and (ii) reaction-limited growth, where the incorporation of building units into the crystal lattice is slower than their diffusion. Ostwald ripening—where larger particles grow at the expense of smaller, more soluble ones—can also occur, leading to a narrowing of the particle size distribution over time[36].

The interplay between thermodynamic parameters (temperature, pressure, pH) and kinetic factors (precursor concentration, reaction time, additives) enables precise tuning of ZnO nanoparticle size, morphology, and crystallinity. This tunability is crucial for investigating size-dependent quantum effects and defect physics in ZnO nanostructures[37].

2. 3. Nucleation, Growth, Quantum Confinement, and Defect Formation in ZnO Nanoparticles

2.3.1. Nucleation and Growth at the Nanoscale

In the hydrothermal synthesis of ZnO, the transition from a supersaturated ionic solution to crystalline nanostructures necessitates a series of physical phenomena—nucleation, growth, and coarsening—each dictated by thermodynamic and kinetic laws[38]. As previously articulated, once the critical threshold of supersaturation is attained, stable nuclei of ZnO are established. At the nanoscale, the elevated surface-to-volume ratio renders surface and interface energies significantly more influential than in bulk materials, thereby affecting not only the rates of nucleation but also the morphology of the resulting crystals[39].

The subsequent growth phase may be modulated through the manipulation of solution chemistry, temperature, and temporal parameters. The incorporation of mineralizers

or capping agents has the potential to selectively adsorb onto specific crystallographic facets, thereby either inhibiting or promoting their growth, which facilitates the customized synthesis of nanorods, nanoplates, or isotropic nanoparticles. The ultimate size and shape distribution of the particles are contingent upon the dynamic interplay of nucleation rates, monomer availability, and ripening mechanisms, including Ostwald ripening and oriented attachment. Understanding the mechanisms of Ostwald ripening in ZnO nanoparticles is crucial, as it directly influences their size distribution and morphological characteristics during synthesis[40], [41].

2.3.2. Quantum Confinement Effects

When the dimensions of ZnO nanoparticles approach or fall below the exciton Bohr radius (~2.34 nm), quantum confinement effects become significant. In this regime, the continuous energy bands of the bulk material split into discrete, size-dependent energy levels. This leads to observable blue shifts in the optical absorption and photoluminescence spectra, a reduction in dielectric screening, and changes in carrier dynamics.

The quantum confinement effect in ZnO nanoparticles can be described by the effective mass approximation (EMA), where the energy shift (ΔE) relative to the bulk bandgap is given by:

$$\Delta E = \frac{h^2\pi^2}{2R^2}\left(\frac{1}{m_e^*}+\frac{1}{m_h^*}\right) - 1.8\frac{e^2}{4\pi\varepsilon_0\varepsilon_r R} \tag{2.3}$$

Where R is the nanoparticle radius, m_e^* and m_h^* are the effective masses of electrons and holes, and ε_r is the relative dielectric constant [42]. This framework allows for a quantitative description of the size-dependent optical properties, which are frequently used to infer nanoparticle dimensions and electronic structure experimentally.

2.3.3. Defect Formation and Physics

At the nanoscale, ZnO is particularly prone to the formation of intrinsic point defects such as oxygen vacancies (V_o), zinc interstitials (Zn_i), oxygen interstitials (O_i), and zinc vacancies (V_{Zn}). These defects can act as shallow donors or deep acceptors, introducing localized electronic states within the bandgap. The concentration and type of defects are sensitive to synthesis parameters including temperature, precursor stoichiometry, and ambient atmosphere[43].

Defect states are fundamental to understanding a variety of physical phenomena in ZnO, including its n-type conductivity, visible luminescence, and surface reactivity. For instance, oxygen vacancies and zinc interstitials are commonly associated with the characteristic green luminescence of ZnO, whereas zinc vacancies can act as deep acceptors, influencing the electrical compensation and magnetic properties of the material. Theoretical studies—often employing density functional theory (DFT)—support the experimental identification of these states and their role in carrier recombination, trapping, and migration[44].

The combination of quantum confinement and defect physics in ZnO nanoparticles results in a complex interplay between structure, electronic states, and optical properties. Understanding these phenomena is essential for the design, optimization, and functionalization of ZnO nanomaterials for both fundamental and applied research[45].

2.4. Characterization Techniques for ZnO Nanoparticles

2.4.1. X-ray Diffraction (XRD)

Principle and Application:

X-ray diffraction, which is widely recognized as a non-destructive analytical technique, serves the purpose of providing detailed insights into the intricate crystal structure, the diverse phase composition, and the average size of crystallites present in nanomaterials, making it an invaluable tool in materials science research. When a carefully controlled monochromatic beam of X-rays engages with a crystalline sample, it gives rise to constructive interference phenomena at particular angles, which can be precisely described and predicted by Bragg's law (see Figure 2.2), thus allowing for

the determination of various structural parameters of the material under investigation [46]:

$$n\lambda = 2dsin(\theta) \tag{2.4}$$

where n is an integer, λ is the X-ray wavelength, d is the interplanar spacing, and θ\thetaθ is the diffraction angle.

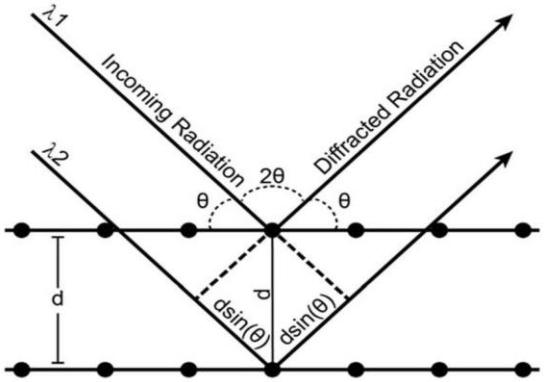

Figure 2.2 Schematic representation of Bragg's law conditions.

The resulting diffraction pattern is characteristic of the atomic arrangement and symmetry within the crystal lattice. The broadening of diffraction peaks can be analyzed using the Scherrer equation to estimate the average crystallite size, which is especially relevant for nanoparticles and can provide insights into the effects of quantum confinement and defect states on their structural properties. Understanding these relationships is crucial for optimizing the synthesis and application of ZnO nanoparticles in various fields [47].

2.4.2 Scanning Electron Microscopy (SEM)

Principle and Application:

Scanning Electron Microscopy (SEM) employs a highly focused and precisely directed beam of high-energy electrons, which meticulously scans the intricate surface of a specimen to gather detailed information. Figure 2.3 illustrates the block diagram of a SEM

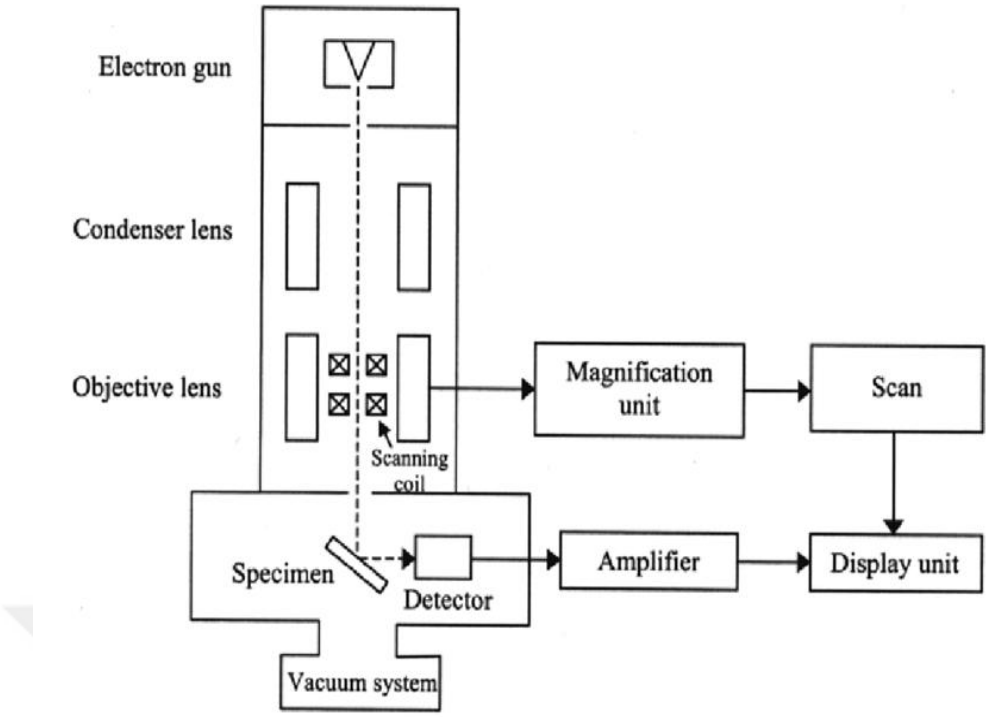

Figure 2.3 Block diagram of a SEM, showing the general layout of the essential components[48].

The dynamic interaction that occurs between these energetic electrons and the constituent atoms of the sample leads to the generation of a variety of signals, including but not limited to secondary electrons and backscattered electrons, which are subsequently collected to produce remarkably high-resolution images that reveal intricate details. SEM proves to be exceptionally effective for the visualization of surface morphology, as well as for analyzing critical parameters such as particle size, shape, and the agglomeration state of various nanoparticles present in the sample. In the realm of research focused on zinc oxide (ZnO) nanomaterials, SEM provides the invaluable capability to directly observe and analyze the diverse morphological features, including nanorods, nanospheres, and other unique structures that arise from specific synthesis conditions and processes. The integration of advanced characterization techniques such as X-ray diffraction (XRD) and scanning electron microscopy (SEM) is essential for comprehensively understanding the structural and morphological properties of ZnO nanoparticles[49], [50].

2.4.3. Raman Spectroscopy

Principle and Application:

Raman spectroscopy, an analytical technique that boasts incredible power and precision, thoroughly delves into and examines the complex vibrational and rotational modes that are displayed by a diverse array of molecules, along with the various crystalline structures, all through the intricate process of inelastic scattering of monochromatic light, a remarkable phenomenon that is commonly accomplished by utilizing a highly concentrated beam of light that is generated by the advanced technology of a laser, which enables such detailed investigations to take place. Figure.2.4 Schematic shows the difference between Stokes and anti-Stokes Raman scattering.

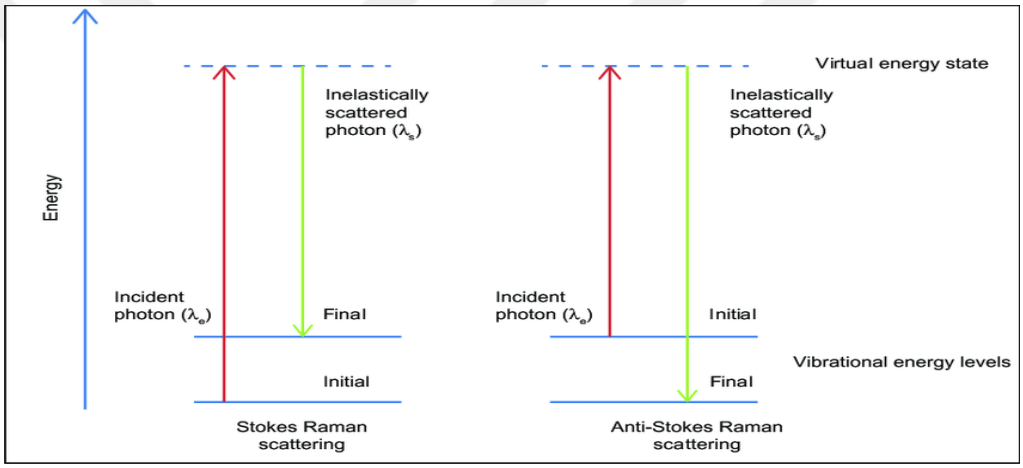

Figure 2.4 The difference between Stokes and anti-Stokes Raman scattering [51].

The combination of Raman spectroscopy with scanning electron microscopy (SEM) allows for comprehensive material analysis, enhancing the understanding of ZnO's structural and electronic properties [52] This multimodal approach is crucial for advancing the characterization of nanomaterials and optimizing their applications in technology. When incident photons interact with the lattice vibrations (phonons) of ZnO, energy is exchanged, resulting in Raman-shifted photons. The spectrum provides fingerprint information about phonon modes, crystal quality, and disorder. In wurtzite ZnO, characteristic Raman peaks such as the E2(high) mode are strong indicators of crystalline quality, while defect- or disorder-induced modes can also appear.[53], [54], [55].

2.4.4. Photoluminescence (PL) Spectroscopy

Principle and Application:

Photoluminescence (PL) spectroscopy, which is an advanced and highly sophisticated scientific technique employed in the realm of materials science, involves a complex process that requires the excitation of electrons within a semiconductor material to remarkably elevated energy levels through the deliberate application of photons, and this intricate process is immediately followed by the emission of light when these excited electrons ultimately recombine with the vacancies referred to as holes that exist within the structure of the material itself. The emission spectrum that results from this multifaceted process not only serves as a vital and essential indicator of the underlying properties of the material but also reflects the intricate band structure of the semiconductor, while simultaneously revealing the presence of various types of defects or irregularities that may exist within the material itself, thereby providing invaluable insights into its overall quality and functionality[56], [57]. In ZnO nanoparticles, PL typically shows a strong ultraviolet (UV) emission due to near-band-edge excitonic recombination, along with possible visible emissions associated with defect levels such as oxygen vacancies[58].

2.4.5. Zeta Potential Measurement

Principle and Application:

The measurement of zeta potential involves the assessment of the electrostatic potential that exists at the slipping plane of a nanoparticle that is suspended within a liquid medium, a process that is essential for gaining insights into the intricate nature of colloidal stability and the various factors that influence it over time. When an electric field is applied to a system, it causes charged particles within that medium to migrate in a process known as electrophoresis, and it is important to note that the velocity of these migrating particles is intricately related to the zeta potential, which serves as a key indicator of their movement. High absolute values of zeta potential, whether they are positive or negative, are indicative of excellent dispersion stability within the system, whereas low zeta potential values suggest a significant tendency for those particles to come together and aggregate, potentially leading to undesirable outcomes in the overall stability of the dispersion. In ZnO nanomaterials, zeta potential provides insights into surface charge, synthesis quality, and suitability for further

functionalization. Understanding the zeta potential of ZnO nanoparticles is crucial for optimizing their stability and performance in various applications, particularly in catalysis and sensor technologies[59], [60].

CHAPTER 3

MATERIALS &METHODS

3.1. Synthesis of ZnO Nanoparticles

Zinc oxide nanoparticles were synthesized using a controlled hydrothermal process. Initially, 0.40 g of zinc acetate dihydrate ($Zn(CH_3COO)_2 \cdot 2H_2O$) was dissolved in 20 mL of deionized water under vigorous magnetic stirring for 15 minutes to obtain a clear and homogeneous precursor solution. In a separate vessel, 0.36 g of sodium hydroxide (NaOH) was dissolved in 20 mL of distilled water, also with continuous stirring, until complete dissolution was achieved.

The NaOH solution was added dropwise to the zinc acetate (see Figure 3.1) solution under constant stirring to ensure uniform mixing and to control the local supersaturation, which is critical for the nucleation process. The resulting mixture was stirred vigorously for an additional hour to facilitate precursor interaction and to promote the formation of initial ZnO nuclei.

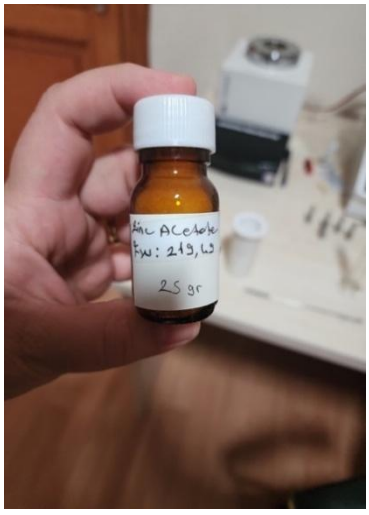

Figure 3.1 The photo of the zinc acetate

Subsequently, the reaction mixture was transferred into a Teflon-lined stainless-steel autoclave, which was securely sealed and placed in a laboratory oven preheated to

170°C. The hydrothermal reaction was maintained at this temperature for a predetermined duration in the system shown in Figure 3.2. After the specified reaction time elapsed, the autoclave was carefully removed and allowed to cool to room temperature by immersion in water at ambient conditions.

Figure 3.2 The hydrothermal system

The resulting white precipitate, consisting of ZnO nanoparticles, was collected by filtration and thoroughly washed several times with deionized water to remove residual ions and unreacted species. The washed product was then dried in a conventional oven at 120°C for 6 hours to obtain a fine powder of ZnO nanoparticles, which was subsequently used for further characterization.

For optimization studies, the hydrothermal synthesis was systematically performed at varying reaction times—namely, 5, 15, 25, and 35 hours—while all other experimental parameters were kept constant. This allowed for the investigation of the effect of reaction duration on nanoparticle size, morphology, and crystallinity.

3.2. Characterization Techniques

3.2.1. Zeta Potential and Particle Size Analysis

The hydrodynamic diameter (agglomeration size) and surface charge (zeta potential) of the synthesized ZnO nanoparticles were determined using a Malvern Nano ZS90 dynamic light scattering (DLS) analyzer. Measurements were performed in aqueous suspension at room temperature to assess colloidal stability and dispersion quality, which are critical parameters for subsequent functional applications.

3.2.2. Photoluminescence (PL) Spectroscopy

Photoluminescence measurements were carried out with a HITACHI F-2500 fluorescence spectrophotometer. The excitation wavelength was set to 371 nm, which is suitable for promoting electron transitions in ZnO. The emission spectra were recorded to analyze band edge emission and defect-related luminescence, providing insights into electronic structure and defect states.

3.3.3 Raman Spectroscopy

Raman spectra were obtained using a Lab RAM HR spectrometer (Jobin Yvon Horiba, France), equipped with a charge-coupled device (CCD) detector. A 632 nm excitation laser and a holographic notch filter were employed. Raman measurements were primarily used to verify the formation of the wurtzite ZnO phase and to assess crystalline quality and phonon characteristics.

3.3.4. Scanning Electron Microscopy (SEM)

The morphology and microstructural features of the ZnO nanoparticles were investigated using a ZEISS EVO scanning electron microscope, operated at an accelerating voltage of 30 kV and equipped with a LaB_6 filament electron source. The microscope provided a nominal resolution of approximately 2 nm and was capable of imaging at magnifications ranging from less than 5× up to 1,000,000×. The maximum sample height was 145 mm.

3.3.5. X-ray Diffraction (XRD)

Crystallographic analysis was performed using a Bruker D8 Advance X-ray diffractometer as seen in Figure 3.3. The instrument was used to collect diffraction patterns over a suitable 2θ range, enabling the identification of ZnO phases, determination of lattice parameters, and estimation of average crystallite size through peak broadening analysis (Scherrer equation).

Figure 3.3 Bruker D8 Advance X-ray diffractometer.

CHAPTER 4

RESULTS & DISCUSSIONS

In this chapter, the structural, morphological, optical, and surface properties of the ZnO nanoparticles synthesized via the hydrothermal method are systematically examined using a range of complementary characterization techniques. The influence of synthesis duration and post-synthesis annealing on the crystalline structure, particle size, crystallinity, and defect states is evaluated in detail. By integrating the results from X-ray diffraction (XRD), scanning electron microscopy (SEM), Raman spectroscopy, photoluminescence (PL) spectroscopy, and zeta potential measurements, a comprehensive understanding of the material evolution is achieved. The following sections present the results and analysis for each technique, starting with the investigation of phase composition and crystallite size via XRD.

4.1. X-ray Diffraction (XRD) Analysis

Figure 4.1 illustrates the X-ray diffraction patterns that correspond to the ZnO nanoparticles, which were meticulously synthesized using the hydrothermal method for a duration of 5 hours, showcasing both the state of the nanoparticles immediately after preparation, referred to as as-prepared (dried), and the state following a controlled annealing process carried out at a temperature of 300°C for a period of 2 hours, all conducted within a nitrogen atmosphere to ensure optimal conditions for structural integrity and phase stabilization of the nanoparticles.

In the as-prepared (dried) sample, broad diffraction peaks are observed at 2θ values of 32.5°, 35.3°, and 37.0°, which are assigned to the (100), (002), and (101) planes of the hexagonal wurtzite ZnO structure (JCPDS card No. 36-1451). The broadness of the peaks, together with their moderate intensity, indicates a relatively small crystallite size and a possible presence of microstrain or structural disorder. Crystallite sizes, calculated using the Scherrer equation, are 11.2 nm for (100), 14.9 nm for (002), and 11.5 nm for (101) reflections.

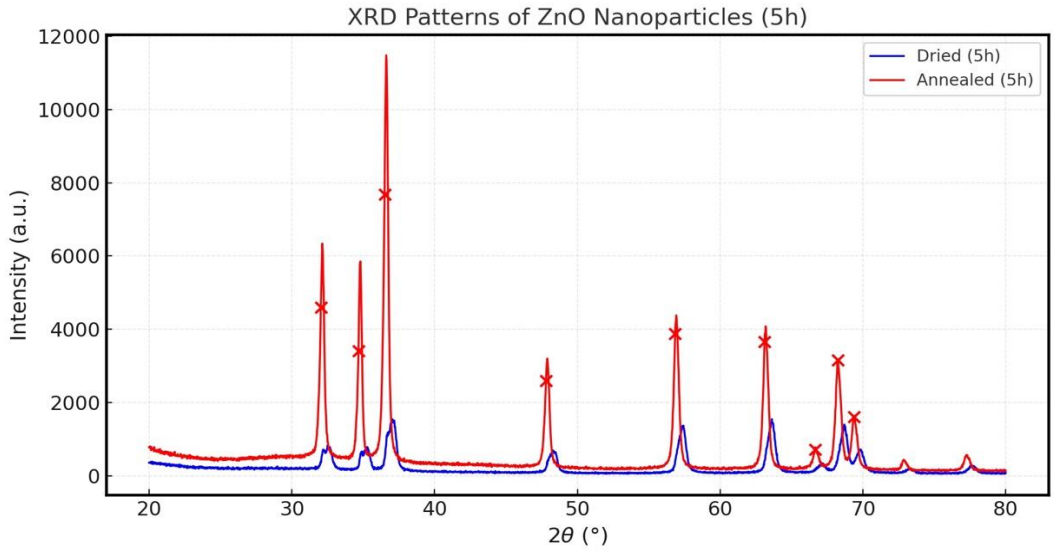

Figure 4.1 XRD patters of ZnO nanoparticles synthesized for 5 Hours.

Upon annealing, the XRD peaks become significantly sharper and more intense. The main diffraction peaks shift slightly to 2θ = 32.1°, 34.8°, and 36.6°, which are still consistent with the (100), (002), and (101) planes of wurtzite ZnO. The calculated crystallite sizes dramatically increase to 29.5 nm (100), 36.9 nm (002), and 29.5 nm (101), indicating substantial crystal growth and improved crystallinity due to thermal treatment. This result also suggests the reduction of defects and possible grain coalescence during annealing. The preservation of peak positions and absence of impurity phases confirm the phase purity of ZnO. These findings are consistent with previous reports that hydrothermally synthesized ZnO nanocrystals show increased crystallinity and grain size after moderate-temperature annealing [61], [62]. Annealing at 300°C effectively promotes atomic diffusion, healing lattice defects and facilitating the growth of well-ordered ZnO nanocrystals.

Figure 4.2 presents the XRD patterns for ZnO samples synthesized for 15 hours, again comparing the as-prepared and annealed states. For the as-prepared sample, diffraction peaks at 2θ = 32.1°, 34.7°, and 36.5° correspond to the (100), (002), and (101) wurtzite planes. The peaks are noticeably sharper and more intense than those of the 5-hour sample, indicating improved crystallinity and a larger average crystallite size. The Scherrer-derived sizes are 23.4 nm (100), 27.0 nm (002), and 23.1 nm (101).

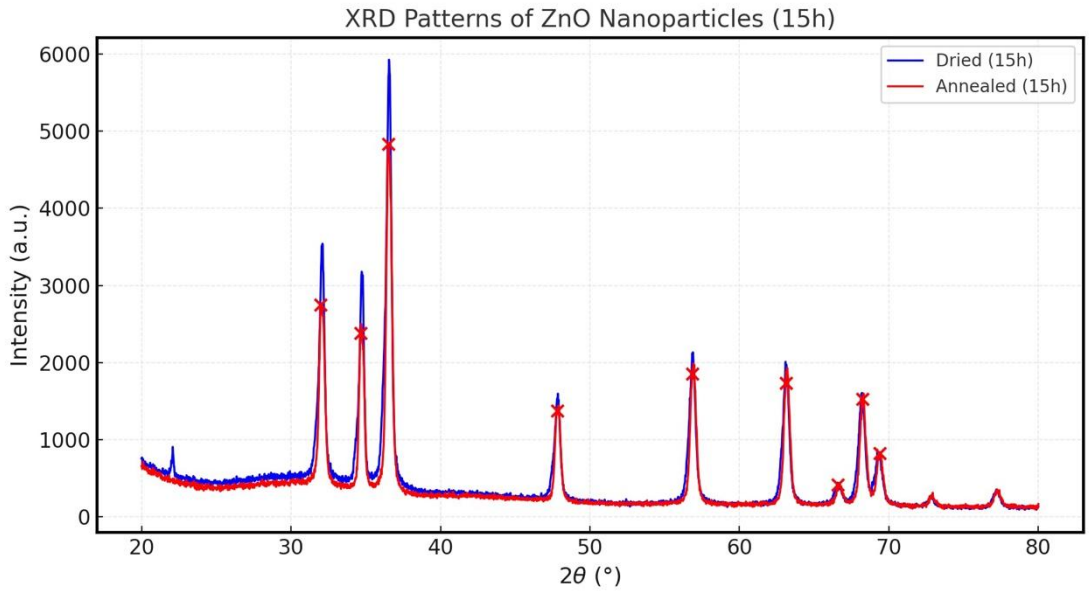

Figure 4.2 XRD patters of ZnO nanoparticles synthesized for 15 Hours.

Unexpectedly, after annealing, the crystallite sizes decrease slightly to 19.2 nm (100), 20.7 nm (002), and 20.1 nm (101), even though the peaks remain sharp and the overall intensity is preserved. The positions of the peaks remain unchanged, and no secondary phases are observed, indicating stable wurtzite structure and phase purity. The reduction in crystallite size may be related to grain boundary relaxation, the elimination of lattice defects, or minor grain fragmentation during the annealing process.

This somewhat counterintuitive decrease in crystallite size after annealing at intermediate synthesis times has also been reported in other nanomaterial systems [63]. It is sometimes attributed to relaxation of internal strains or mild grain refinement processes that can occur during post-synthesis thermal treatment, especially when the initial particle size is already substantial.

Figure 4.3 shows the XRD patterns for samples synthesized for 25 hours, before and after annealing. The as-prepared sample exhibits strong, sharp peaks at 2θ = 31.9°, 34.6°, and 36.4°, again corresponding to the (100), (002), and (101) planes of hexagonal ZnO. The crystallite sizes are calculated as 26.8 nm (100), 40.6 nm (002), and 27.4 nm (101), indicating a high degree of crystallinity and larger average grain size relative to the 5-hour and 15-hour samples.

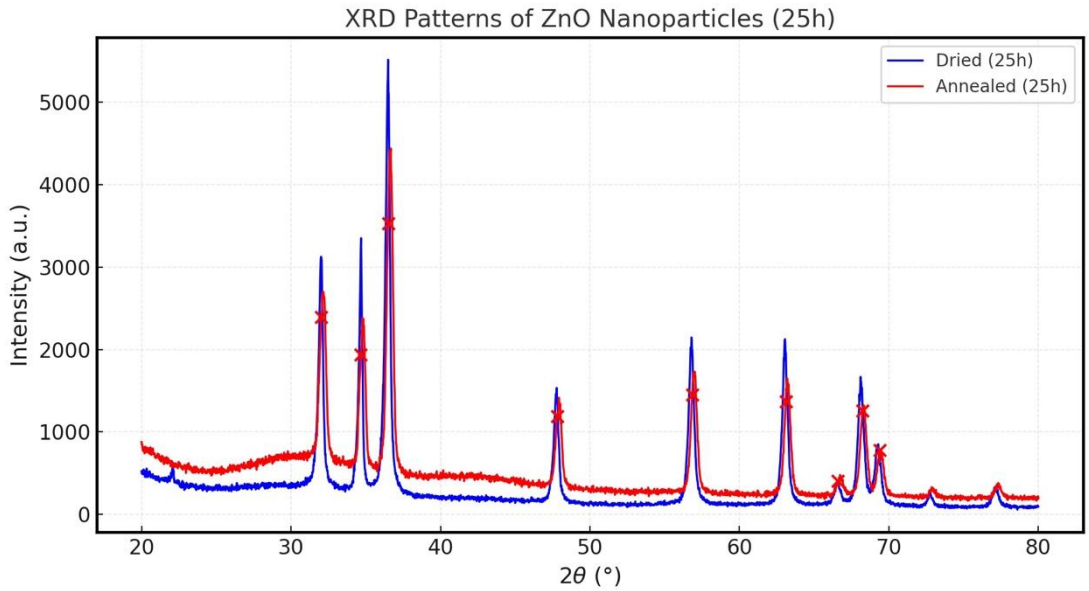

Figure 4.3 XRD patters of ZnO nanoparticles synthesized for 25 Hours.

After annealing, there is a reduction in the calculated crystallite sizes to 17.8 nm (100), 19.7 nm (002), and 18.3 nm (101). Despite this decrease, the peaks remain sharp, and phase purity is maintained. The observed reduction may again be linked to grain refinement or the release of internal lattice stresses.

Such behavior, where annealing can cause either coalescence or refinement depending on initial nanocrystal size and defect content, is recognized in the literature [64]. It underscores the complex interplay between crystal growth and defect dynamics during post-synthesis thermal treatments.

Figure 4.4 displays the XRD patterns for ZnO samples synthesized for 35 hours. The as-prepared sample exhibits relatively sharp diffraction peaks at 2θ = 32.3°, 35.0°, and 36.8° (wurtzite ZnO planes), with calculated crystallite sizes of 24.2 nm (100), 23.2 nm (002), and 21.4 nm (101). After annealing, both peak sharpness and intensity increase further, with the largest calculated crystallite sizes among all samples: 32.7 nm (100), 36.3 nm (002), and 31.7 nm (101).

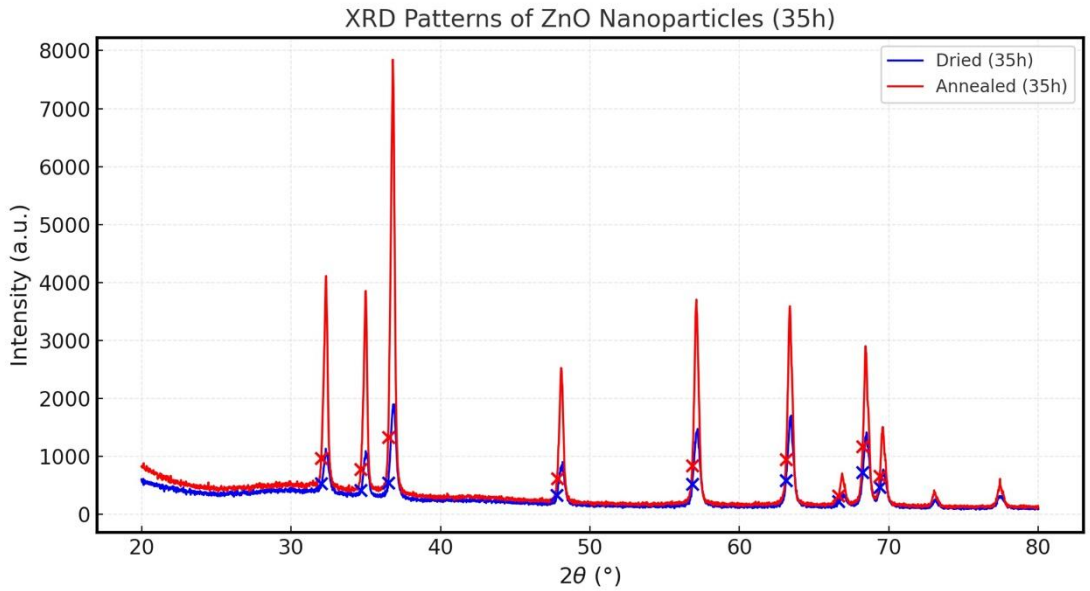

Figure 4.4 XRD patters of ZnO nanoparticles synthesized for 35 Hours.

No new peaks or impurity phases are observed. The substantial increase in crystallite size and crystallinity upon annealing at 35 hours indicates optimal conditions for defect healing and domain growth in the ZnO lattice.

The synergistic effect of extended hydrothermal synthesis and annealing aligns with previous work showing that combining long reaction times with moderate thermal post-treatment yields highly crystalline, defect-free ZnO nanomaterials [61], [62].

Analysis of the crystallite size trends reveals that annealing leads to a significant increase in crystallite size for the 5-hour and 35-hour samples, indicative of substantial grain growth and effective defect reduction, whereas for the 15-hour and 25-hour samples, annealing results in a modest decrease in crystallite size, which may be attributed to strain relaxation or minor grain refinement processes.

Across all samples, irrespective of synthesis duration or post-treatment, the XRD patterns exhibit only the characteristic peaks of the hexagonal wurtzite ZnO phase, confirming the high phase purity of the materials. Notably, the 35-hour annealed sample displays the sharpest and most intense peaks, reflecting the highest degree of crystallinity and the most well-developed crystal structure among the examined samples. These observations are consistent with established literature, which emphasizes that both synthesis duration and annealing play critical roles in the structural evolution of hydrothermally prepared ZnO nanoparticles, with annealing generally promoting crystal growth and defect reduction, although the precise effects are dependent on the initial microstructural state of the material [61], [62], [63], [64].

To gain further insight into the morphology, particle size, and aggregation behavior of the synthesized ZnO nanoparticles, SEM analysis was performed, as presented in the following section.

4.2. Scanning Electron Microscopy (SEM) Analysis

Figure 4.5 illustrates scanning electron microscopy (SEM) micrographs of zinc oxide (ZnO) nanoparticles that were synthesized via hydrothermal methods for varying durations: (a) 5 hours, (b) 15 hours, (c) 25 hours, and (d) 35 hours. All depicted images are presented at a uniform magnification (scale bar: 1 μm), thereby facilitating an explicit comparison of particle morphology and aggregation characteristics across the different samples.

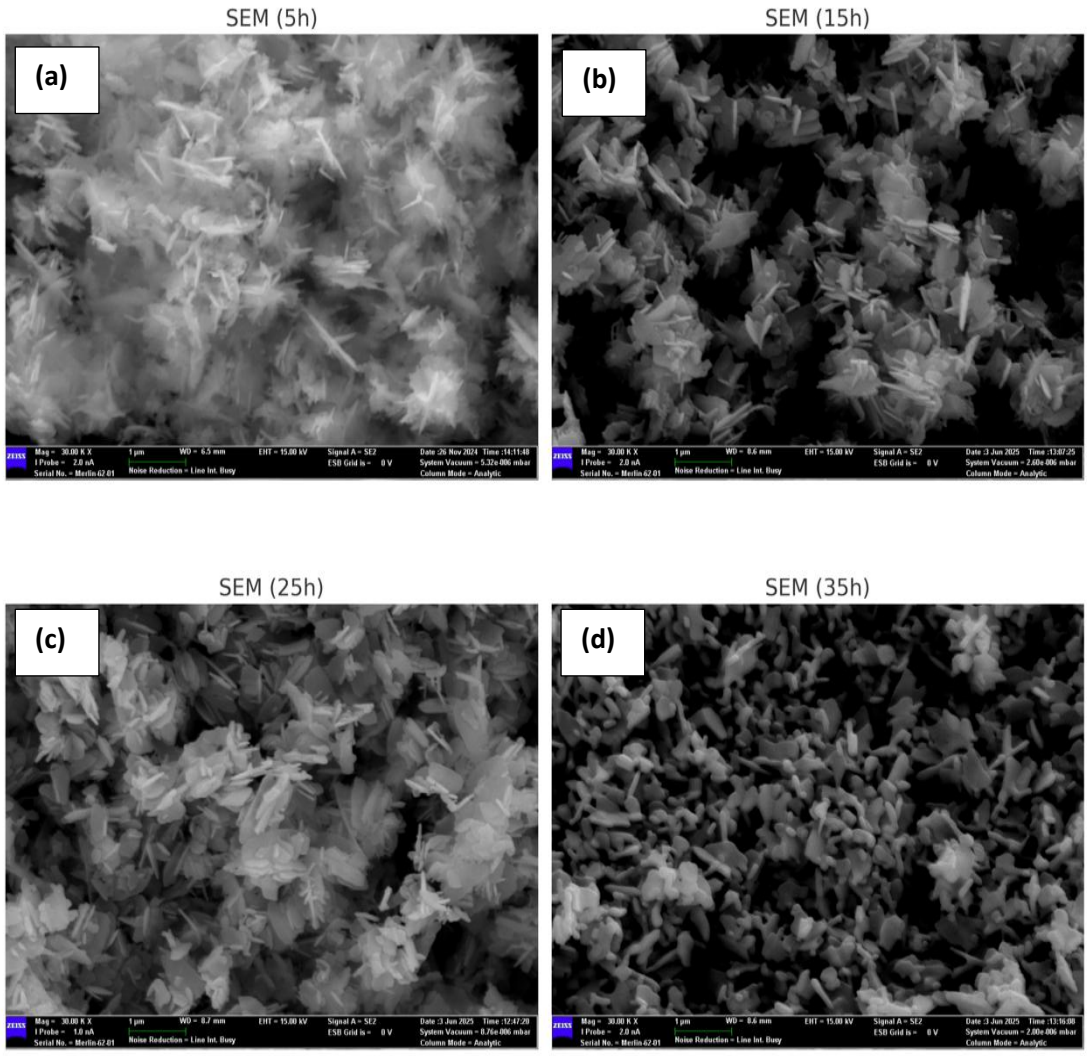

Figure 4.5 SEM micrographs of ZnO nanoparticles synthesized for (a) 5 Hours, (b)15 Hours, (c) 25 Hours and (d) 35 Hours.

For the sample synthesized for 5 hours (Figure 4.5.a), the microstructure is characterized by densely packed, flower-like aggregates composed of numerous nanoscale rod- or plate-shaped primary particles. These structures exhibit considerable intergrowth and overlap, resulting in a high degree of agglomeration and limited separation between individual crystallites. The primary particles appear relatively short and thick, with estimated lengths on the order of 200–400 nm and widths of approximately 50–100 nm, though some variation is present due to overlapping features.

With increasing synthesis time to 15 hours (Figure 4.5.b), the ZnO particles maintain a similar flower-like morphology but become more distinctly developed, with better-defined individual rods or plates radiating outward from central points. The agglomeration persists, yet the inter-particle separation is slightly improved compared to the 5-hour sample. The primary rods/plates appear longer and somewhat thinner, suggesting ongoing growth and possible anisotropic crystal development during extended hydrothermal processing.

In the 25-hour sample (Figure 4.5.c), the flower-like aggregates remain the dominant morphological motif; however, the individual rods and plates become even more prominent, and the assemblies are more open, indicating partial reduction in agglomeration. The rods display increased aspect ratios, and the average particle size continues to grow modestly. These features suggest that prolonged synthesis enables continued growth and slight coarsening of the nanostructures, while still promoting self-assembly into hierarchical morphologies[65].

The 35-hour sample (Figure 4.5d) reveals a notable evolution in morphology. The micrograph displays a more dispersed arrangement, with the flower-like structures partially breaking down into smaller, less interconnected rod- or needle-like particles. The degree of agglomeration is further reduced, and the overall particle distribution appears more uniform. Many of the rods are well separated, and the background matrix is less dense, indicating that very long hydrothermal reaction times favor the formation of discrete nanorods or nanoneedles over highly aggregated flower-like assemblies.

These morphological trends are consistent with previous studies on hydrothermal ZnO synthesis, where reaction time is a key factor in determining particle size, shape, and

aggregation behavior [66], [67]. The observed progression—from densely packed flower-like aggregates at shorter synthesis times to more open, less agglomerated structures at longer durations—can be attributed to Ostwald ripening, anisotropic growth along specific crystallographic axes, and partial breakdown of hierarchical assemblies with extended reaction[68]. This morphological evolution complements the XRD results, which indicate increased crystallite size and crystallinity for longer synthesis times, as well as reduced defect density. The combination of flower-like and rod/needle-like morphologies is characteristic of hydrothermal ZnO, and their control

4.3. Raman Spectroscopy Analysis

Figure 4.6 presents the Raman spectrum of ZnO nanoparticles synthesized for 5 hours. The spectrum is dominated by a strong E_2 *(high)* mode at ~439 cm^{-1}, a well-established signature of the wurtzite ZnO phase and high crystallinity [70], [71].

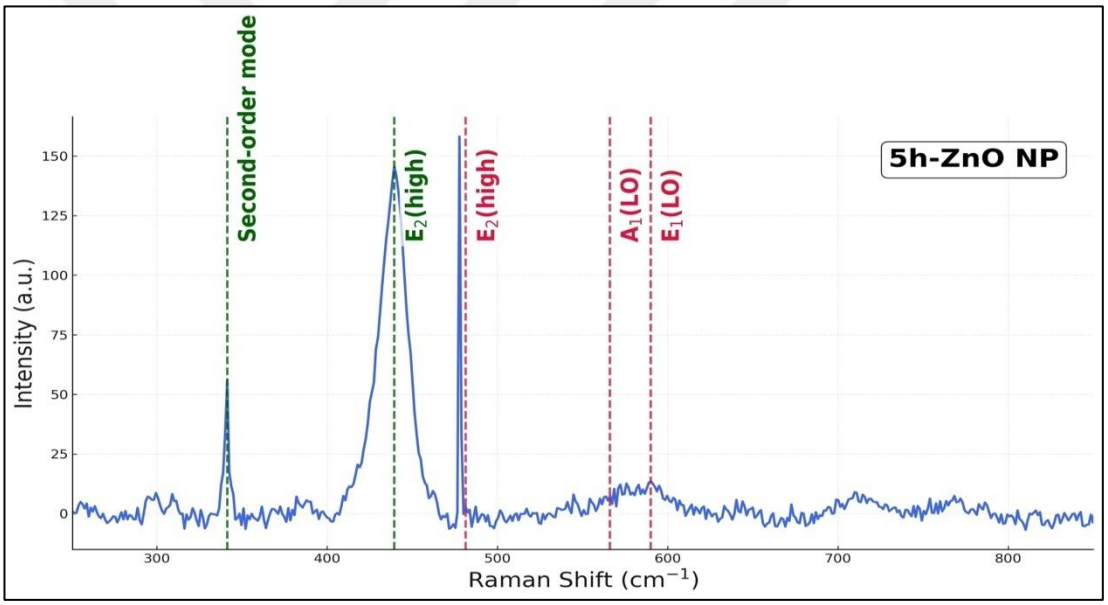

Figure 4.6 The Raman spectrum of ZnO nanoparticles synthesized for 5 hours.

A second-order phonon mode is observed at ~341 cm^{-1}, further supporting the presence of good crystalline order. The appearance of a shifted E_2 *(high)* peak at ~481 cm^{-1}, typical for nanostructures, is attributed to phonon confinement, internal stress, and size effects[72], [73]. Additionally, longitudinal optical (*LO*) modes A_1 *(LO)* at ~566 cm^{-1} and E_1 *(LO)* at ~590 cm^{-1} are visible, both of which are sensitive to defects, non-stoichiometry, and carrier concentration. The pronounced intensity of the E_2 *(LO)*

and *LO* modes confirms nanostructured ZnO with high crystallinity, while the presence and shift of these modes indicate the influence of nanostructuring and lattice imperfections.

These results are in good agreement with previous reports, which show strong E_2 *(LO)* peaks as an indicator of phase-pure, crystalline ZnO and the sensitivity of *LO* modes to nanoscale effects and defect states [70], [71], [72], [73].

Figure 4.7 shows the Raman spectrum for the 15-hour sample. The E_2 *(high)* peak appears at ~439 cm^{-1} but exhibits a slight shift, which may be due to stress or quantum confinement effects associated with nanostructuring.

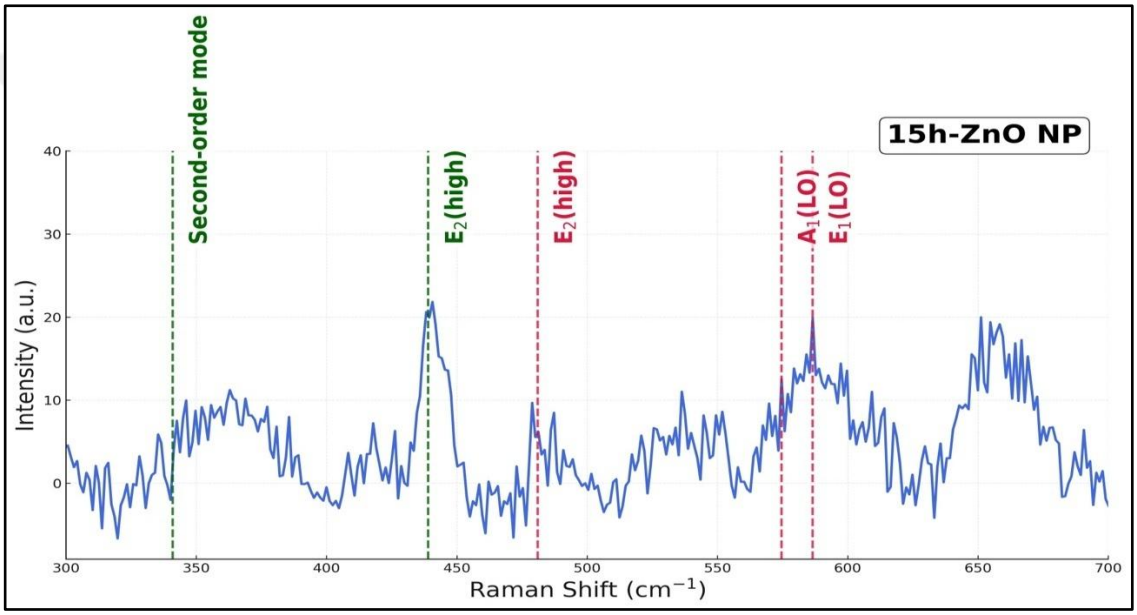

Figure 4.7 The Raman spectrum of ZnO nanoparticles synthesized for 15 hours.

The second-order mode at ~341 cm^{-1} is still present, indicating continued high crystalline quality. The nano-shifted E_2 *(high)* peak at ~481 cm^{-1}, as in the 5-hour sample, further supports the presence of phonon confinement and strain effects [74]. The A_1 *(LO)* and E_1 *(LO)* modes at ~575 cm^{-1} and ~587 cm^{-1}, respectively, are also present, providing evidence for surface states, lattice disorder, and defect-related phenomena.

The clear signatures of wurtzite ZnO and the observed peak shifts are consistent with the expected behavior for nanostructured ZnO, where defect states and quantum confinement become more pronounced as particle size decreases [72], [73], [74].

Figure 4.8 presents the Raman spectrum for ZnO nanoparticles synthesized over 25 hours. The spectrum continues to show a strong E_2 *(high)* mode at ~439 cm^{-1}, confirming the well-ordered wurtzite structure. A shifted E_2 *(high)* peak is again observed at ~481 cm^{-1}, while the A_1 *(LO)* and E_1 *(LO)* modes at ~576 cm^{-1} and ~590 cm^{-1}, respectively, are indicative of the presence of surface defects and non-stoichiometry. The overall spectral features point to a highly crystalline material with prominent nanostructure-induced effects, such as confinement and surface disorder.

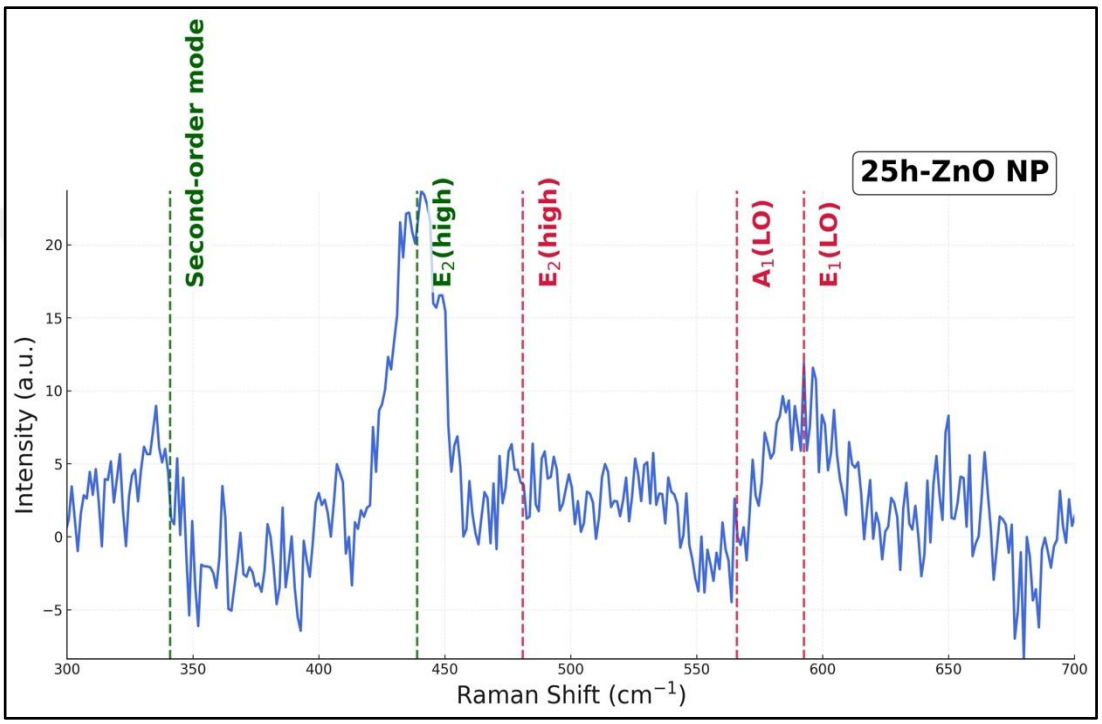

Figure 4.8 The Raman spectrum of ZnO nanoparticles synthesized for 25 hours.

These results further validate that hydrothermal synthesis reliably produces phase-pure ZnO nanostructures, with characteristic Raman signatures matching those reported for high-quality, defect-influenced ZnO nanoparticles [72], [73].

Figure 4.9 displays the Raman spectrum for the 35-hour sample. The E_2 *(high)* mode at ~439 cm^{-1} remains the most intense peak, demonstrating strong crystallinity and preservation of the wurtzite ZnO phase. The shifted E_2 *(high)* feature at ~481 cm^{-1} is pronounced, and the LO modes A_1 *(LO)* and E_1 *(LO)* at ~576 cm^{-1} and ~590 cm^{-1}, respectively, are also evident. The strong LO features reflect an increased surface-to-volume ratio and surface disorder, characteristic of nanomaterials. The spectrum shows all expected modes for nanostructured ZnO, including those related to lattice imperfections and high surface area.

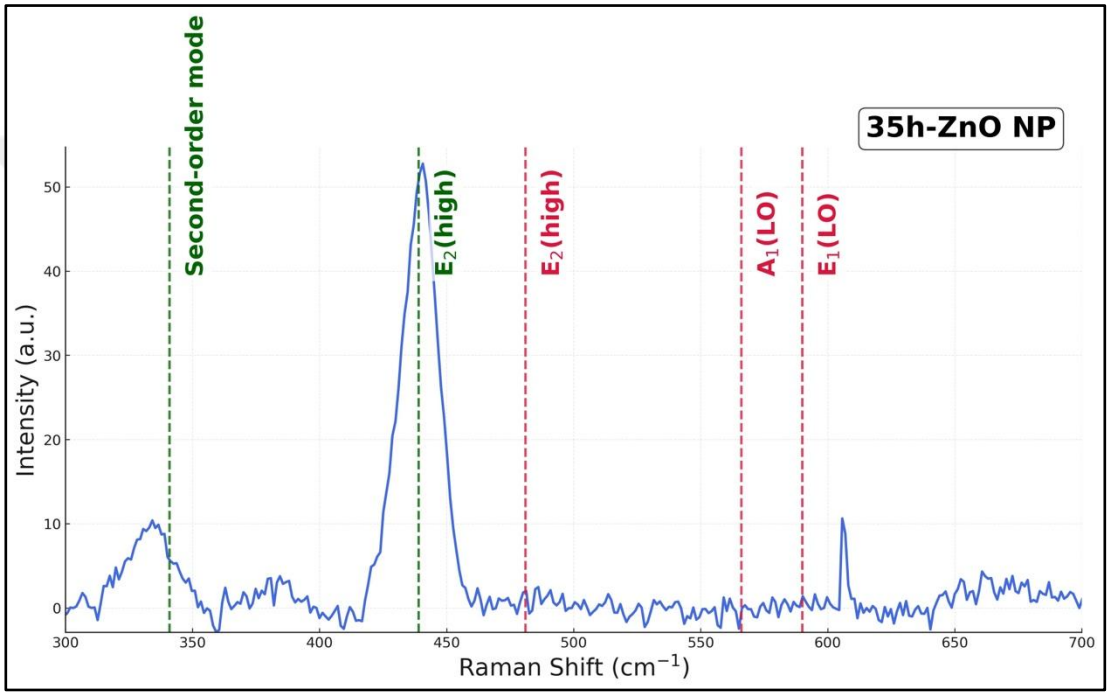

Figure 4.9 The Raman spectrum of ZnO nanoparticles synthesized for 35 hours.

The persistence of all major vibrational modes and their evolution with synthesis duration are in excellent agreement with prior studies on hydrothermal ZnO nanomaterials [71], [72], [73], [74], which also report enhanced surface and defect-related features at the nanoscale.

Table 4.1 Comparative Raman Analysis of ZnO Nanoparticles.

Sample	E_2(high) (cm^{-1})	Shifted E_2(high) (cm^{-1})	A_1(LO) (cm^{-1})	E_1(LO) (cm^{-1})	Comments
5h	~439 [70]	~481 [73]	~566 [70,71]	~590 [70,71]	High crystallinity, strong nanostructure effects, surface/lattice defects
15h	~439 (shifted)	~481 [73]	~575 [70,71]	~587 [70,71]	Wurtzite phase, clear nano-shifts, pronounced LO modes
25h	~439 [70,71]	~481 [73]	~576 [70,71]	~590 [70,71]	Well-ordered, strong stress and confinement effects, high surface states
35h	~439 [70,71]	~481 [73]	~576 [70,71]	~590 [70,71]	Highest crystallinity, clear phase purity, strong nanostructure signatures

As seen from table 4.1, across all samples, the Raman analysis consistently reveals the presence of the wurtzite ZnO phase, strong crystallinity, and clear effects of nanostructuring, including phonon confinement and defect-related phenomena. The evolution of *LO* modes and the appearance of shifted E_2 *(high*) features corroborate the XRD and SEM findings, confirming the successful synthesis of high-quality, nanostructured ZnO and highlighting the interplay between synthesis conditions, particle size, and defect states.

4.4. Zeta Potential Analysis

Table 4.2 summarizes the average zeta potential values (in mV) for ZnO nanoparticles synthesized at different hydrothermal reaction times (5h-10-25 and 35 h)

As seen from the table, all samples display highly negative zeta potential values (from -22.9 mV to -29.6 mV). And, there is no significant monotonic trend with synthesis duration; the values remain within a similar range, with the 5-hour sample exhibiting slightly more negative values on average. In addition, standard deviations are low, suggesting that the synthesis is highly reproducible and the nanoparticles exhibit consistent surface charge behavior.

Table 4.2 Zeta potential values (in mV) with Standart Deviation (Std. Deviation) for ZnO nanoparticles synthesized for 5h-10-25 and 35 h.

Sample	Mean Zeta Potential (mV)	Std. Deviation (mV)	n(number of measurements)
ZnO (5 h)	-26.4	2.46	5
ZnO (15 h)	-24.8	0.73	5
ZnO (25 h)	-25.1	0.29	5
ZnO (35 h)	-25.7	0.94	5

As seen from the table, all samples display highly negative zeta potential values (from -22.9 mV to -29.6 mV). And, there is no significant monotonic trend with synthesis duration; the values remain within a similar range, with the 5-hour sample exhibiting slightly more negative values on average. In addition, standard deviations are low, suggesting that the synthesis is highly reproducible and the nanoparticles exhibit consistent surface charge behavior. A negative zeta potential indicates that the surface of the ZnO nanoparticles acquires a net negative charge when dispersed in aqueous media. This negative charge primarily arises from the adsorption of hydroxyl ions (OH^-) onto the nanoparticle surfaces, as well as from the deprotonation of surface-bound hydroxyl groups [75], [76]. Such surface chemistry is characteristic of metal oxide nanoparticles in neutral or slightly basic environments, where the presence of negatively charged species in the electrical double layer leads to a net negative surface potential[77], [78].

The sign and magnitude of the zeta potential are crucial parameters for predicting colloidal stability. Nanoparticles with zeta potential values greater than ±25 mV generally possess sufficient electrostatic repulsion to overcome attractive van der Waals forces, thereby inhibiting aggregation and promoting stable dispersions In this study, all ZnO samples exhibited zeta potentials near or below -25 mV, confirming their strong electrostatic stabilization and high colloidal stability in water[78], [79]. This behavior is beneficial for applications where long-term dispersion and minimal particle aggregation are required, such as in nanofluids, photocatalysis, and biomedical formulations.

The one-way analysis of variance (ANOVA) is a statistical method used to determine whether there are any statistically significant differences between the means of three or more independent groups. One-way ANOVA was conducted to test whether the synthesis duration has a significant effect on zeta potential. In the context of ANOVA, the *F value* (or *F statistic*) is a ratio that compares the variance between group means to the variance within the groups; a higher *F* value typically suggests a greater difference between group means relative to the variation within groups. The *p value* indicates the probability that the observed difference among group means occurred by random chance; a p value less than 0.05 is commonly interpreted as statistically significant, whereas a larger p value suggests no significant difference among the groups[80].

ANOVA results showed no significant difference in mean zeta potential values among ZnO samples with different synthesis durations ($F = 0.44,\ p = 0.73$). The results indicate no statistically significant difference between the groups ($F = 0.44$**,** $p = 0.73$), confirming that hydrothermal reaction time, within the studied range, does not appreciably affect the surface charge of ZnO nanoparticles.

4.5. Photoluminescence (PL) Analysis

Figure 4.10 presents a comprehensive depiction of the photoluminescence (PL) spectra associated with zinc oxide (ZnO) nanoparticles that have been meticulously synthesized under a diverse range of hydrothermal reaction durations, specifically at intervals of 5 hours, 15 hours, 25 hours, and 35 hours, and this analysis is conducted under two distinctly different monochromator slit widths, which are set at 20 and 10. In Figure 4.10(a), one can observe the PL response that corresponds to the slit width of 20, whereas in the Figure 4.10(b), the spectra that have been meticulously acquired at the narrower slit width of 10 are presented for comparison. For each of these specified slit widths, the intensity of the PL is meticulously delineated as a function of the emission wavelength, thus enabling a thorough and detailed comparison of both the signal intensity and the distinctive spectral characteristics across all of the various synthesis periods that have been explored.

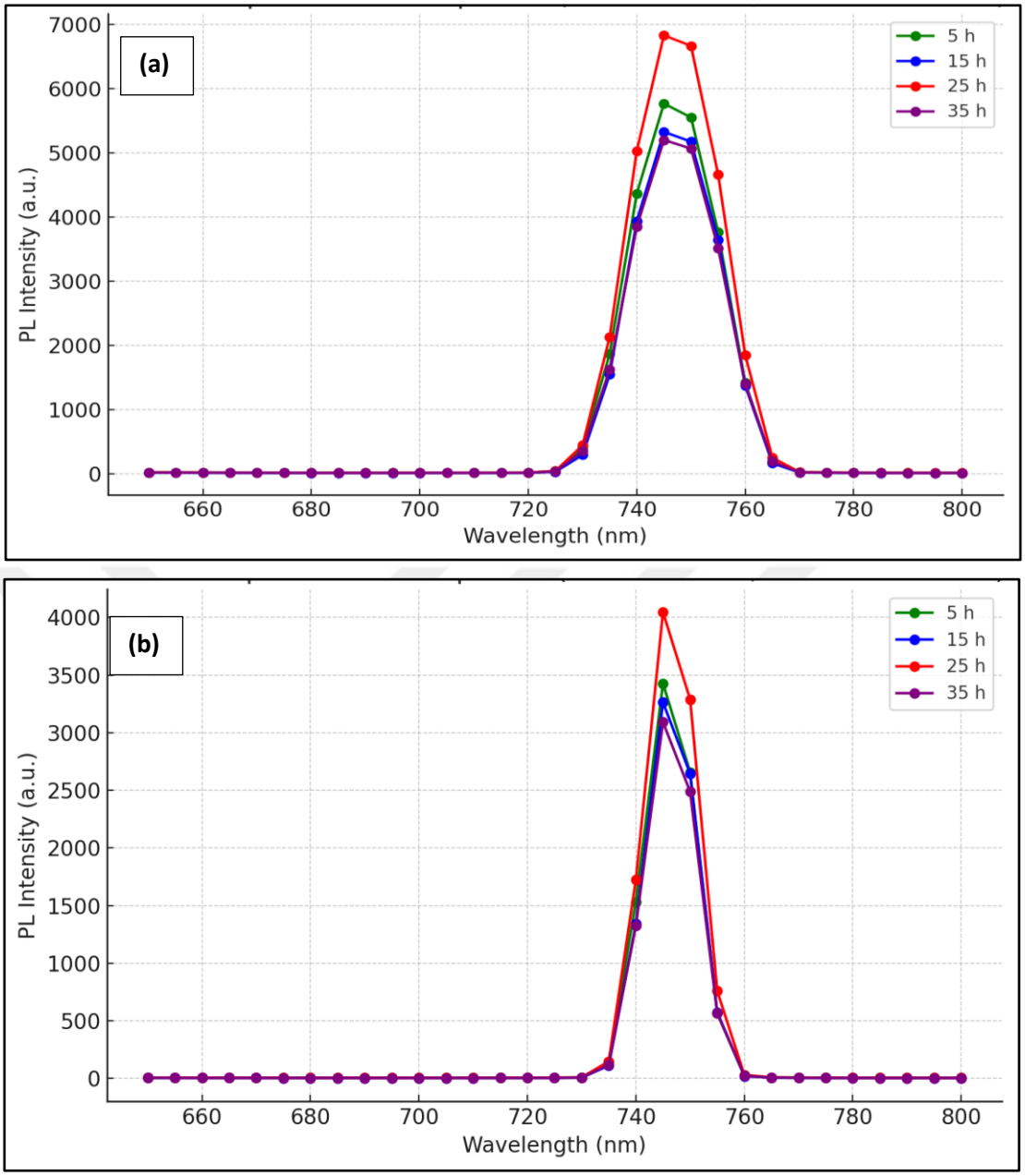

Figure 4.10 Photoluminescence (PL) spectra of zinc oxide (ZnO) nanoparticles synthesized at different hydrothermal reaction times (5 h, 15 h, 25 h, and 35 h), measured using (a) a 20-slit width and (b) a 10-slit width.

For both slit widths, all samples exhibit a prominent emission band centered around 740–745 nm. This emission lies in the near-infrared region and is generally attributed, in the context of ZnO nanostructures, to deep-level or defect-related states, such as oxygen vacancies or zinc interstitials. Notably, the intensity and sharpness of the emission vary with both synthesis time and slit width.

At a 20-slit width (see Figure 4.10(a)), the PL intensity increases progressively from 5 h to 25 h, reaching a maximum for the 25-hour sample, before decreasing slightly for the 35-hour sample. The peak is sharpest and most intense for the 25-hour ZnO, suggesting either an optimal concentration of radiative recombination centers or the presence of a well-developed defect structure at this synthesis duration. The 5-hour and 15-hour samples display lower intensities and slightly broader peaks, possibly reflecting smaller crystallite sizes and higher levels of non-radiative defects, as supported by XRD and SEM results.

With a 10-slit width (see Figure (4.10(b)), a similar trend is observed: PL intensity is highest for the 25-hour sample, with other samples following the same order as in the 20-slit case. The overall intensity is reduced, as expected due to the narrower slit, but the relative changes among the samples remain consistent. The sharper emission peaks at the narrower slit also indicate the intrinsic spectral characteristics of the ZnO nanoparticles.

These results highlight the strong dependence of PL emission on both synthesis duration and measurement conditions. The evolution of PL intensity with synthesis time is likely governed by the competition between defect formation and crystal quality: as synthesis duration increases, defect-related radiative centers may increase up to an optimal point (25h), after which further growth and annealing can lead to the reduction or passivation of these centers, thus reducing PL intensity. This trend aligns with the observed changes in crystallite size, morphology, and defect density reported in the XRD and SEM analyses.

Such near-infrared defect emission is widely reported for ZnO nanomaterials synthesized via wet-chemical and hydrothermal methods [81], [82], [83]. The dependence of PL intensity on synthesis duration is often linked to the interplay between surface states, defect concentration, and particle size. Studies show that emission intensity can peak at intermediate growth stages, where an optimal balance exists between crystallinity and defect density, and then decrease as further crystal growth reduces available defect sites or facilitates non-radiative recombination [82], [84].

Overall, the PL spectra provide valuable information about the optical properties and defect structure of the ZnO nanoparticles, supporting and extending the findings from structural and morphological analyses. The pronounced, tunable PL emission suggests potential for these materials in optoelectronic or sensing applications where defect-mediated luminescence is beneficial.

In addition to the spectral photoluminescence measurements, photographic evidence of ZnO nanoparticle dispersions under ambient and excitation conditions is provided in Figure 4.11**.** The images clearly demonstrate the visible photoluminescence of the ZnO nanoparticles when suspended in water and exposed to UV light.

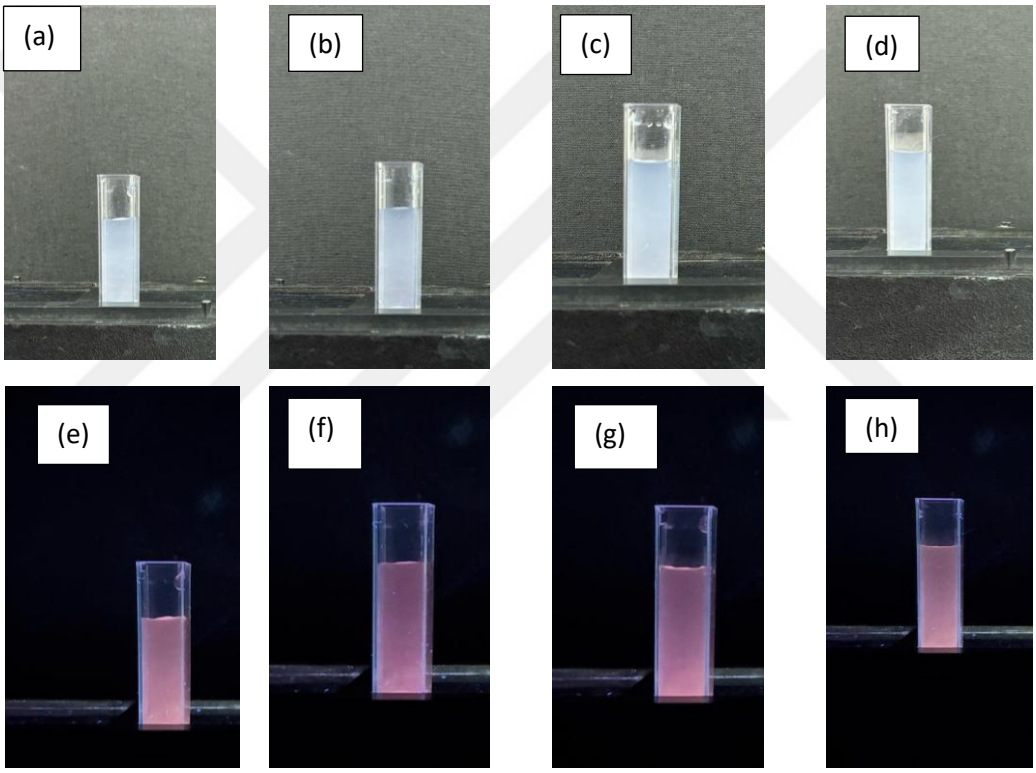

Figure 4.11 Photographs of ZnO nanoparticle dispersions in water under (a–d) ambient light and (e–h) UV excitation. Images (a) and (e): 5 h; (b) and (f): 15 h; (c) and (g): 25 h; (d) and (h): 35 h synthesis durations, respectively (from left to right).

Under normal illumination (Figures 4.11 a, b, c, d), the dispersions appear milky-white or faintly bluish, characteristic of colloidal ZnO in water. Upon UV or optical excitation (Figures 4.11 e, f, g, h), all samples exhibit a distinct pink-red luminescence, corresponding to the deep-level emission observed in the PL spectra. The emission is visually intense and uniformly distributed throughout the cuvette, confirming the homogeneous dispersion and efficient radiative recombination in the colloidal state.

Notably, the emission color is most vivid for the 25-hour sample, consistent with the maximum PL intensity observed in the spectral data. This qualitative visual evidence reinforces the quantitative trends identified in the PL measurements, further supporting the conclusion that synthesis duration strongly influences defect-related emission in hydrothermally synthesized ZnO nanoparticles.

Such visible emissions from ZnO colloids are widely reported in the literature and is generally associated with oxygen vacancies and surface states, which act as radiative centers [85], [86]. The strong pink-red emission highlights the potential of these nanoparticles for applications in bioimaging, sensing, and optoelectronics, where solution-phase luminescence is a key requirement.

CHAPTER 5

CONCLUSION

This thesis successfully demonstrated the fabrication of zinc oxide (ZnO) nanoparticles via a hydrothermal method and systematically investigated the effect of synthesis duration (5, 15, 25, and 35 hours) on their resulting properties. The comprehensive characterization of the synthesized nanoparticles has led to the following key conclusions:

1. **Structural Properties:** The hydrothermal method was effective in producing phase-pure ZnO nanoparticles with a hexagonal wurtzite crystal structure, as confirmed by XRD analysis across all samples. A clear trend was observed where longer synthesis times, especially when combined with post-synthesis annealing, led to enhanced crystallinity and larger crystallite sizes. The sample synthesized for 35 hours and subsequently annealed exhibited the highest degree of crystallinity, indicating that extended reaction times promote a more ordered crystal lattice.

2. **Morphological Evolution:** SEM analysis revealed a significant evolution in nanoparticle morphology as a function of reaction time. The synthesis progressed from forming dense, flower-like aggregates at shorter durations (5 hours) to producing more discrete and well-defined rod- or needle-like particles at longer durations (35 hours). This transition, likely driven by mechanisms such as Ostwald ripening and anisotropic growth, highlights that the reaction duration is a powerful tool for controlling the shape and agglomeration state of ZnO nanostructures.

3. **Optical and Vibrational Properties:** Raman spectroscopy consistently confirmed the high quality of the wurtzite phase in all samples, identified by the prominent E_2(high) mode. Photoluminescence (PL) studies showed that all nanoparticles exhibit a strong, defect-mediated emission in the near-infrared region (~740 nm), which corresponds to a visible pink-red luminescence under

UV excitation. Notably, the PL intensity reached its maximum at an intermediate synthesis time of 25 hours, suggesting that this duration provides an optimal balance between the formation of radiative defect centers and the maintenance of high crystal quality.

4. **Colloidal Stability:** Zeta potential measurements indicated that all synthesized ZnO nanoparticle samples possess high colloidal stability in aqueous dispersion. The consistently high negative surface charge (around -25 mV) across all samples demonstrates a strong electrostatic repulsion that prevents aggregation. Statistical analysis (ANOVA) confirmed that the synthesis duration, within the studied range, did not have a significant impact on the surface charge of the nanoparticles.

In summary, this research successfully establishes a clear correlation between the hydrothermal synthesis duration and the structural, morphological, and optical properties of ZnO nanoparticles. By carefully tuning the reaction time, it is possible to control particle morphology from complex aggregates to discrete nanorods and to optimize their photoluminescent properties. The high purity, crystallinity, and excellent colloidal stability of the synthesized nanoparticles make them promising candidates for a variety of advanced applications, including photocatalysis, sensing, bioimaging, and optoelectronic devices. Future work could focus on further optimizing other synthesis parameters (e.g., temperature, pH, precursor concentration) and evaluating the performance of these tailored nanoparticles in specific device applications.

REFERENCES

[1] V. L. Ranganatha, K. S. Nithin, S. A. Khanum, G. Nagaraju, and C. Mallikarjunaswamy, "Zinc oxide nanoparticles: A significant review on synthetic strategies, characterization and applications," *AIP Conference Proceedings*, 2019, p. 020089.

[2] P. K. Mishra, H. Mishra, A. Ekielski, S. Talegaonkar, and B. Vaidya, "Zinc oxide nanoparticles: a promising nanomaterial for biomedical applications," *Drug Discovery Today*, vol. 22, no. 12, pp. 1825–1834, Dec. 2017.

[3] R. Verma, S. Pathak, A. K. Srivastava, S. Prawer, and S. Tomljenovic-Hanic, "ZnO nanomaterials: Green synthesis, toxicity evaluation and new insights in biomedical applications," *Journal of Alloys and Compounds*, vol. 876, p. 160175, Sep. 2021.

[4] G. E. Yenorkar, "Insights into Structural and Optical Properties of ZnO Nanoparticles," International Journal for Research in Applied Science and Engineering Technology, vol. 12, no. 6, pp. 1437–1440, Jun. 2024.

[5] M. R. Ghahfarokhi, M. Alizadeh Pirposhte, D. Mukherjee, A. J. Dehaghani, J. Amirian, A. Brangule, and D. Bandere, "Nano ZnO: Structure, Synthesis Routes, and Properties," *Book Chapter*, in *ZnO and Their Hybrid Nano-Structures: Potential Candidates for Diverse Applications*, Materials Research Foundations, Vol. 146, 2023, pp. 1–34.

[6] T. Asaulyuk, Y. Saribyekova, O. Semeshko, and I. Kulish, "Synthesis and Structural Characterization of ZnO Nanoparticles," *Herald of Khmelnytskyi National University. Technical Sciences*, vol. 311, no. 4, pp. 35–41, Aug. 2022.

[7] L. Shen, E. Y. B. Pun, and J. C. Ho, "Recent developments in III–V semiconducting nanowires for high-performance photodetectors," *Materials Chemistry Frontiers*, vol. 1, no. 4, pp. 630–645, 2017.

[8] X. Chen and H. Zhang, "A Bandgap-optimization-induced Sensitivity Enhancement Effect in a Novel Ionization Gas Sensor with Composite Nanostructure," in *2022 International Conference on Applied Physics and Computing (ICAPC)*, IEEE, Sep. 2022, pp. 328–331.

[9] J. Theerthagiri et al., "A review on ZnO nanostructured materials: energy, environmental and biological applications," *Nanotechnology*, vol. 30, no. 39, p. 392001, Sep. 2019.

[10] T. K. Mandal, “ZnO Nanoparticles: Sustainable Plant Production,” in *Sustainable Agriculture Reviews*, Springer, Cham, 2024, pp. 259–281.

[11] R. R. Gandhi and D. K. Koche, “An Insight of Zinc Oxide Nanoparticles (ZnO NPs): Green Synthesis, Characteristics and Agricultural Applications,” *Biosciences Biotechnology Research Asia*, vol. 21, no. 3, pp. 863–876, Sep. 2024.

[12] C. Pushpalatha et al., “Zinc Oxide Nanoparticles: A Review on Its Applications in Dentistry,” *Frontiers in Bioengineering and Biotechnology*, vol. 10, May 2022.

[13] S. Bhosale, N. Kannor, N. Shinde, and N. Sahane, “Recent Advances in Zinc Oxide Nanoparticles: Synthesis Methods, Characterization Techniques, and Emerging Applications,” *Current Catalysis*, vol. 13, no. 2, Jan. 2025.

[14] B. A. Aderibigbe, *“Zinc Oxide Nanoparticles in Biomedical Applications: Advances in Synthesis, Antimicrobial Properties, and Toxicity Considerations,”* Book Chapter, in *Nanotechnology in the Life Sciences: Nanoparticles in Modern Antimicrobial and Antiviral Applications*, Springer International Publishing, 2024, pp. 119–149.

[15] P. Pandey, R. Kurchania, and F. Z. Haque, “Controlled hydrothermal synthesis, structural and optical analysis of nanometer-sized ZnO spheres,” *Optik*, vol. 126, no. 2, pp. 301–303, Jan. 2015.

[16] K. Żelechowska, “Methods of ZnO nanoparticles synthesis,” *BioTechnologia*, vol. 95, no. 2, pp. 150–159, Jan. 2015.

[17] S. Wirunchit and W. Koetniyom, “ZnO Nanoparticles Synthesis and Characterization by Hydrothermal Process for Biological Applications,” *Physica Status Solidi (a)*, vol. 220, no. 10, May 2023.

[18] S.-H. Hu, Y.-C. Chen, C.-C. Hwang, C.-H. Peng, and D.-C. Gong, “Analysis of growth parameters for hydrothermal synthesis of ZnO nanoparticles through a statistical experimental design method,” *Journal of Materials Science*, vol. 45, no. 19, pp. 5309–5317, Oct. 2010.

[19] A. B. Djurisic, Y. Y. Xi, Y. F. Hsu, and W. K. Chan, “Hydrothermal Synthesis of Nanostructures,” *ChemInform*, vol. 38, no. 41, Oct. 2007.

[20] R. Suryanarayanan, “Zinc Oxide: From Optoelectronics to Biomaterial—A Short Review,” in *Functional Materials*, Springer, 2014, pp. 289–307.

[21] X. Gu, C. Li, S. Yuan, M. Ma, Y. Qiang, and J. Zhu, “ZnO based heterojunctions and their application in environmental photocatalysis,” *Nanotechnology*, vol. 27, no. 40, p. 402001, Oct. 2016.

[22] F. Bosi, G. B. Andreozzi, U. Halenius, and H. Skogby, “Zn-O tetrahedral bond length variations in normal spinel oxides,” *American Mineralogist*, vol. 96, no. 4, pp. 594–598, Apr. 2011.

[23] R. Tan, Y.-L. Zhang, Y. Yang, W. Song, T. Xu, and Q. Nie, “Pyroelectric properties of ZnO-based nanostructured polycrystalline ceramics,” in *Proc. SPIE 7381, Nanoengineering: Fabrication, Properties, Optics, and Devices VI*, vol. 7381, p. 738120, Jul. 2009.

[24] X. Pengshou, S. Yuming, S. Chaoshu, X. Faqiang, and P. Haibin, “Electronic structure of ZnO and its defects,” *Science in China Series A: Mathematics*, vol. 44, no. 9, pp. 1174–1181, Sep. 2001.

[25] Q. Yang, L. Tong, and Z. L. Wang, “Nanophotonic Devices Based on ZnO Nanowires,” in *Three-Dimensional Nanoarchitectures*, New York, NY: Springer, 2011, pp. 317–362.

[26] Md. N. Hossain, M. H. Chowdhury, Md. J. Islam, and T. S. Akhter, “Analysis of the properties of ZnO nanoparticle for emerging applications in nanoscale domains,” in *2013 IEEE 56th International Midwest Symposium on Circuits and Systems (MWSCAS)*, pp. 928–931, Aug. 2013.

[27] D. K. Sharma, S. Shukla, K. K. Sharma, and V. Kumar, “A review on ZnO: Fundamental properties and applications,” *Materials Today: Proceedings*, vol. 49, pp. 3028–3035, 2022.

[28] S. Nadupalli, S. Repp, S. Weber, and E. Erdem, “About defect phenomena in ZnO nanocrystals,” *Nanoscale*, vol. 13, no. 20, pp. 9160–9171, 2021.

[29] J. Callaway and A. J. Hughes, “Localized defects in semiconductors,” *International Journal of Quantum Chemistry*, vol. 1, no. S1, pp. 769–771, Jun. 2009.

[30] J. L. Gomez and O. Tigli, “Zinc oxide nanostructures: from growth to application,” *Journal of Materials Science*, vol. 48, no. 2, pp. 612–624, Jan. 2013.

[31] A. R. Rachamim, S. H. Dalal, S. M.-L. Pfaendler, M. E. Swanwick, A. Flewitt, and W. I. Milne, “Quantitative Investigation of the Factors Affecting the Hydrothermal Growth of Zinc Oxide Nanowires,” *MRS Proceedings*, vol. 1174, p. V11-08, Jan. 2009.

[32] F. Demoisson, R. Piolet, and F. Bernard, “Hydrothermal Synthesis of ZnO Crystals from $Zn(OH)_2$ Metastable Phases at Room to Supercritical Conditions,” *Crystal Growth & Design*, vol. 14, no. 11, pp. 5388–5396, Nov. 2014.

[33] M. Ethayaraja, K. Dutta, and R. Bandyopadhyaya, “Mechanism of Nanoparticle Formation in Self-Assembled Colloidal Templates: Population Balance Model and Monte Carlo Simulation,” *Journal of Physical Chemistry B*, vol. 110, no. 33, pp. 16471–16481, Aug. 2006.

[34] S.-W. Chen and J.-M. Wu, “Nucleation mechanisms and their influences on characteristics of ZnO nanorod arrays prepared by a hydrothermal method,” *Acta Materialia*, vol. 59, no. 2, pp. 841–847, Jan. 2011.

[35] Y. Tong et al., “Growth of ZnO Nanostructures with Different Morphologies by Using Hydrothermal Technique,” *Journal of Physical Chemistry B*, vol. 110, no. 41, pp. 20263–20267, Oct. 2006.

[36] W. Sun, “Particle coarsening: I. Kinetics for reversible dissolution/deposition controlled process,” *Acta Materialia*, vol. 53, no. 11, pp. 3329–3334, Jun. 2005.

[37] M. M. Ba-Abbad, A. A. H. Kadhum, A. B. Mohamad, M. S. Takriff, and K. Sopian, “The effect of process parameters on the size of ZnO nanoparticles synthesized via the sol–gel technique,” *Journal of Alloys and Compounds*, vol. 550, pp. 63–70, Feb. 2013.

[38] W.-J. Li, E.-W. Shi, Y.-Q. Zheng, and Z.-W. Yin, “Hydrothermal preparation of nanometer ZnO powders,” *Journal of Materials Science Letters*, vol. 20, no. 15, pp. 1381–1383, 2001.

[39] S. V. Karpenko and A. I. Temrokov, “On the role of surface energy in nanodimensional crystalline objects,” *Technical Physics*, vol. 49, no. 11, pp. 1509–1511, Nov. 2004.

[40] V. P. Zhdanov, E. M. Larsson, and C. Langhammer, “Novel aspects of Ostwald ripening of supported metal nanoparticles,” *Chemical Physics Letters*, vol. 533, pp. 65–69, Apr. 2012.

[41] N. Wang, L. Jiang, H. Peng, and G. Li, "Synthesis of ZnO nanostructures composed of nanosheets with controllable morphologies," *Crystal Research and Technology*, vol. 44, no. 3, pp. 341–345, Mar. 2009.

[42] Z. D. Fu, Y. Q. Wang, D. H. Zhang, and G. S. Yang, “Study on the quantum confinement effect on ultraviolet photoluminescence of crystalline ZnO nanoparticles with nearly uniform size,” *Applied Physics Letters*, vol. 90, no. 26, p. 263113, Jun. 2007.

[43] D. Q. Fang and R. Q. Zhang, “Size effects on formation energies and electronic structures of oxygen and zinc vacancies in ZnO nanowires: A first-principles study,” *Journal of Applied Physics*, vol. 109, no. 4, p. 044306, Feb. 2011.

[44] F. Oba, M. Choi, A. Togo, and I. Tanaka, "Point defects in ZnO: an approach from first principles," *Science and Technology of Advanced Materials*, vol. 12, no. 3, p. 034302, Jun. 2011.

[45] K. Kitamura, T. Yatsui, and M. Ohtsu, "Observation of quantum confinement in ZnO nanorods fabricated using a two-temperature growth method," *Applied Physics B*, vol. 97, no. 4, pp. 825–828, Dec. 2009.

[46] Y. Xiao, Z. Cai, Z. L. Wang, B. Lai, and Y. S. Chu, "An X-ray nanodiffraction technique for structural characterization of individual nanomaterials," *Journal of Synchrotron Radiation*, vol. 12, no. 2, pp. 124–128, Mar. 2005.

[47] P. Whitfield and L. Mitchell, "X-ray diffraction analysis of nanoparticles: recent developments, potential problems and some solutions," *International Journal of Nanoscience*, vol. 3, no. 6, pp. 757–763, Dec. 2004.

[48] K. Nagarathnam and K. Komvopoulos, "Microstructural characterization and in situ transmission electron microscopy analysis of laser-processed and thermally treated Fe-Cr-W-C clad coatings," *Metallurgical Transactions A*, vol. 24, no. 7, pp. 1621–1629, Jul. 1993.

[49] D. C. Joy, "Introduction to the scanning electron microscope," *Microscopy and Microanalysis*, vol. 9, no. S02, pp. 1556–1557, Aug. 2003.

[50] T. H. Mubarak, K. H. Hassan, and Z. M. A. Abbas, "Using X-ray diffraction and scanning electron microscope to study zinc oxide nanoparticles prepared by wet chemical method," *Advanced Materials Research*, vol. 685, pp. 119–122, Apr. 2013.

[51] W. Wang, H. McGregor, M. Short, and H. Zeng, "Clinical utility of Raman spectroscopy: current applications and ongoing developments," *Advances in Healthcare Technology*, p. 13, Jun. 2016.

[52] G. Wille, X. Bourrat, N. Maubec, and A. Lahfid, "Raman-in-SEM, a multimodal and multiscale analytical tool: Performance for materials and expertise," *Micron*, vol. 67, pp. 50–64, Dec. 2014.

[53] M. Šćepanović, M. Grujić-Brojčin, K. Vojisavljević, S. Bernik, and T. Srećković, "Raman study of structural disorder in ZnO nanopowders," *Journal of Raman Spectroscopy*, vol. 41, no. 9, pp. 914–921, Sep. 2010.

[54] C. H. Ahn, S. K. Mohanta, N. E. Lee, and H. K. Cho, “Enhanced exciton–phonon interactions in photoluminescence of ZnO nanopencils,” *Applied Physics Letters*, vol. 94, no. 26, p. 263103, Jun. 2009.

[55] J. Qu and X. Liu, "Recent advances on SEM-based in situ multiphysical characterization of nanomaterials," *Scanning*, vol. 2021, pp. 1–16, Jun. 2021.

[56] S. Sanguinetti, M. Guzzi, E. Gatti, and M. Gurioli, "Photoluminescence characterization of structural and electronic properties of semiconductor quantum wells," in *Characterization of Semiconductor Heterostructures and Nanostructures*, Elsevier, 2013, pp. 509–556.

[57] P. J. Kempen, C. Hitzman, L. S. Sasportas, S. S. Gambhir, and R. Sinclair, "Advanced characterization techniques for nanoparticles for cancer research: Applications of SEM and NanoSIMS for locating Au nanoparticles in cells," *MRS Proceedings*, vol. 1569, pp. 157–163, May 2013.

[58] G. J. Lee et al., "Photoluminescence and lasing properties of ZnO nanorods," *Journal of the Korean Physical Society*, vol. 57, no. 6(1), pp. 1624–1629, Dec. 2010.

[59] A. Serrano-Lotina, R. Portela, P. Baeza, V. Alcolea-Rodriguez, M. Villarroel, and P. Ávila, "Zeta potential as a tool for functional materials development," *Catalysis Today*, vol. 423, p. 113862, Nov. 2023.

[60] M. T. Connah, M. Kaszuba, and A. Morfesis, "High resolution zeta potential measurements: analysis of multi-component mixtures," *Journal of Dispersion Science and Technology*, vol. 23, no. 5, pp. 663–669, Jan. 2002.

[61] S. Baruah and J. Dutta, “Hydrothermal growth of ZnO nanostructures,” *Science and Technology of Advanced Materials*, vol. 10, no. 1, p. 013001, Jan. 2009.

[62] Ü. Özgür, Y. I. Alivov, C. Liu, A. Teke, M. A. Reshchikov, S. Doğan, et al., “A comprehensive review of ZnO materials and devices,” *Journal of Applied Physics*, vol. 98, no. 4, p. 041301, Aug. 2005.

[63] T. M. Hammad, J. K. Salem, and R. G. Harrison, “The influence of annealing temperature on the structure, morphologies and optical properties of ZnO nanoparticles,” *Superlattices and Microstructures*, vol. 47, no. 2, pp. 335–340, Feb. 2010.

[64] S. Sanjeev and D. Kekuda, “Effect of Annealing Temperature on the Structural and Optical Properties of Zinc Oxide (ZnO) Thin Films Prepared by Spin Coating Process,” *IOP Conference Series: Materials Science and Engineering*, vol. 73, p. 012149, Feb. 2015.

[65] W. Zhang et al., "Formation of rod-like nanostructure by aggregation of TiO_2 nanoparticles with improved performances," *Bulletin of Materials Science*, vol. 38, no. 6, pp. 1617–1623, Oct. 2015.

[66] K. Natrchalayuth, T. Wasanapiarnpong, S. Larpkiattaworn, and P. Sujaridworakun, "Hydrothermal Synthesis of Zinc Oxide Nanoparticle from Zinc-Dust Waste for Photocatalytic and Antibacterial Applications," *Advanced Materials Research*, vol. 506, pp. 78–81, Apr. 2012.

[67] Y. Tong et al., "Growth of ZnO Nanostructures with Different Morphologies by Using Hydrothermal Technique," *Journal of Physical Chemistry B*, vol. 110, no. 41, pp. 20263–20267, Oct. 2006.

[68] H. Chun Zeng, "Ostwald Ripening: A Synthetic Approach for Hollow Nanomaterials," *Current Nanoscience*, vol. 3, no. 2, pp. 177–181, May 2007.

[69] H. Q. Wang et al., "Controlled Hydrothermal Synthesis of ZnO Nano and Microstructure Materials with Photocatalytic Properties," *Advanced Materials Research*, vol. 217–218, pp. 1212–1217, Mar. 2011.

[70] C. Klingshirn, "ZnO: From basics towards applications," *physica status solidi (b)*, vol. 244, no. 9, pp. 3027–3073, Sep. 2007.

[71] Z. L. Wang, "Zinc oxide nanostructures: growth, properties and applications," *Journal of Physics: Condensed Matter*, vol. 16, no. 25, pp. R829–R858, Jun. 2004.

[72] P. Galinetto et al., "Phase stability and homogeneity in undoped and Mn-doped $LiFePO_4$ under laser heating," *Journal of Raman Spectroscopy*, vol. 41, no. 10, pp. 1276–1282, Oct. 2010.

[73] C. Jagadish and S. J. Pearton, *Zinc Oxide Bulk, Thin Films and Nanostructures: Processing, Properties, and Applications*. Amsterdam: Elsevier, 2006.

[74] R. Verma, S. Pathak, A. K. Srivastava, S. Prawer, and S. Tomljenovic-Hanic, "ZnO nanomaterials: Green synthesis, toxicity evaluation and new insights in biomedical applications," *Journal of Alloys and Compounds*, vol. 876, p. 160175, Sep. 2021.

[75] R . J. Hunter, *Zeta Potential in Colloid Science: Principles and Applications*, Academic Press, London,

[76] D. J. Pochapski, C. Carvalho dos Santos, G. W. Leite, S. H. Pulcinelli, and C. V. Santilli, "Zeta Potential and Colloidal Stability Predictions for Inorganic Nanoparticle Dispersions: Effects of Experimental Conditions and

Electrokinetic Models on the Interpretation of Results," *Langmuir*, vol. 37, no. 45, pp. 13379–13389, Nov. 2021.

[77] S. S. A. An, J. Kim, H. Park, and S. Kim, "Physicochemical properties of surface charge-modified ZnO nanoparticles with different particle sizes," *International Journal of Nanomedicine*, vol. 9, pp. 41–50, Dec. 2014.

[78] N. Wang, C. Hsu, L. Zhu, S. Tseng, and J.-P. Hsu, "Influence of metal oxide nanoparticles concentration on their zeta potential," *Journal of Colloid and Interface Science*, vol. 407, pp. 22–28, Oct. 2013.

[79] F. I. Talens-Alesson, "Test for Estimation of Relative Stability of Suspensions by Measure of ζ-Potential," *Chemical Engineering Technology*, vol. 24, no. 2, p. 185, Feb. 2001.

[80] L. Pace, "One-Way Analysis of Variance," in *Beginning R*, Berkeley, CA: Apress, 2012, pp. 139–147.

[81] S. Baruah and J. Dutta, "Hydrothermal growth of ZnO nanostructures," *Science and Technology of Advanced Materials*, vol. 10, no. 1, p. 013001, Jan. 2009.

[82] K. Vanheusden, W. L. Warren, C. H. Seager, D. R. Tallant, J. A. Voigt, and B. E. Gnade, "Mechanisms behind green photoluminescence in ZnO phosphor powders," *Journal of Applied Physics*, vol. 79, no. 10, pp. 7983–7990, May 1996.

[83] B. Liu and H. C. Zeng, "Hydrothermal Synthesis of ZnO Nanorods in the Diameter Regime of 50 nm," *Journal of the American Chemical Society*, vol. 125, no. 15, pp. 4430–4431, Apr. 2003.

[84] A. B. Djurišić and Y. H. Leung, "Optical Properties of ZnO Nanostructures," *Small*, vol. 2, no. 8–9, pp. 944–961, Aug. 2006.

[85] A. Mohanta, V. Singh, and R. K. Thareja, "Photoluminescence from ZnO nanoparticles in vapor phase," *Journal of Applied Physics*, vol. 104, no. 6, Sep. 2008.

[86] V. T. Karpuhin, M. M. Malikov, T. I. Borodina, G. E. Val'yano, and O. A. Gololobova, "Investigation of the characteristics of a colloidal solution and its solid phase obtained through ablation of zinc in water by high-power radiation from a copper vapor laser," *High Temperature*, vol. 49, no. 5, pp. 679–684, Oct. 2011.